
High-Symmetry Low-Coordinate Complexes of Cerium(III) and Uranium(III): Tris[bis(trimethylsilyl)amido] Phosphine Oxide Compounds for Empirical *f*-Element Electronic Structure Investigations

Stewart B. Younger-Mertz

Department of Chemistry, University of Oklahoma, Norman, OK 73019

Donna J. Nelson

Department of Chemistry, University of Oklahoma, Norman, OK 73019

Abstract: This work reports the synthesis and characterization of trivalent four-coordinate tris(silylamido) phosphine oxide complexes of Uranium and Cerium with approximate C_3 symmetry. The pseudo- C_3 symmetric four-coordinate tris[bis(trimethylsilyl)amido] triphenylphosphine oxide framework has only been reported for La, Sm, Eu, Er, Lu, Y, and U. Only the Lanthanum and Uranium derivatives have been characterized by X-ray crystallography, and ^{31}P NMR spectra have only been reported for the diamagnetic derivatives (La and Y). To our knowledge, *f*-element tris(silylamido) phosphine oxide complexes with substituted-aryl phosphine oxide ligands have not been characterized via XRD or NMR. Substituted aryl-derivatives exhibit different reactivities and spectroscopic properties than the simple triphenylphosphine oxide framework, because the relative electron densities on the phosphorus and oxygen atoms are highly influenced by the electronic character of the organic substituents bound to the phosphorus. The nature of the organic substituents on phosphorus therefore highly influences the nature of the metal-oxygen bond in phosphine oxide coordination complexes. These axially symmetric four-coordinate silylamido phosphine oxide complexes are suitable models for studying the relative differences in Ln/An metal-ligand covalency using ^{31}P -NMR spectroscopy and X-ray emission spectroscopy. Expanding this structural framework to other Lanthanide and Actinide metals, and fully characterizing a series of pseudoisomorphous complexes featuring various organic substituents on the phosphine oxide (beyond triphenylphosphine oxide), would provide considerable insight concerning phosphine oxide bonding interactions with *f*-block metals. In addition to being convenient ligands for spectroscopic studies of *f*-element electronic structure, phosphine oxides (and the details of their interactions with *f*-block metals) are directly relevant to the nuclear fuel cycle. The fundamental nature of *f*-block metal phosphine oxide bonds is not well understood, and deeper empirical insight into the nature of these interactions is needed in order to facilitate large-scale computational screening of potential extractants for trivalent Ln/An separations. Herein we report the synthesis, X-ray crystallography, and paramagnetic NMR spectroscopy of a series of trivalent Cerium and Uranium tris(silylamido) phosphine oxide complexes, as well as the X-ray and gamma emission spectra for $\text{Ce}[\text{N}(\text{SiMe}_3)_2]_3[\text{OPPh}_3]$. It was observed in this work that phosphine oxide coordination to the metal center increases the length of the metal-amide bond, which could perhaps explain the enhanced protonolysis reactivity with HPPH_2 that was observed decades ago for lanthanide tris(silylamido) phosphine oxide complexes, compared to their corresponding three-coordinate $\text{Ln}[\text{N}(\text{SiMe}_3)_2]_3$ analogues.

*Corresponding author: djnelson@ou.edu

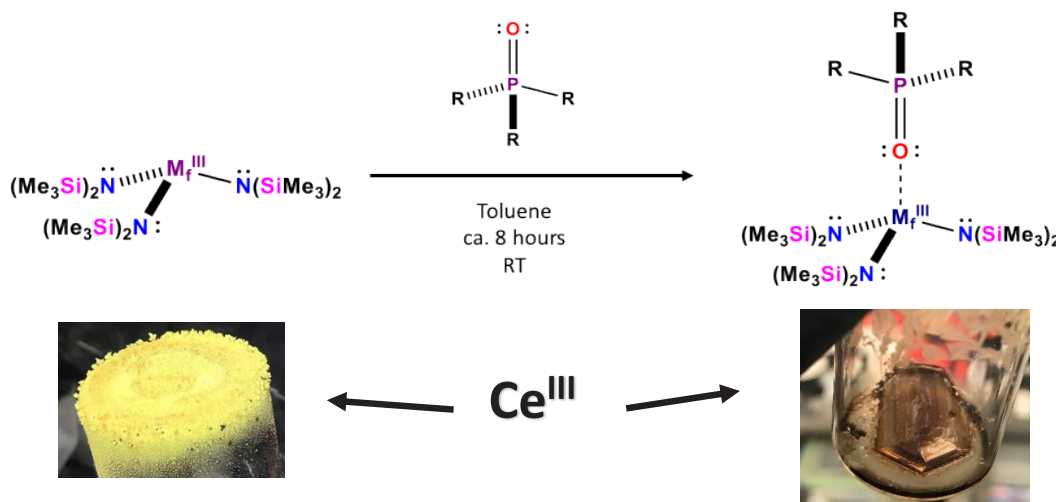
Introduction

This work reports the synthesis and characterization of trivalent four-coordinate tris(silylamide) phosphine oxide complexes of uranium and cerium with approximate C_3 symmetry. Cerium and uranium, along with the rest of the lanthanide and actinide elements, are considered “hard” Lewis acids and have large ionic radii [1-9]. The coordination chemistry of these elements is dominated by high coordination numbers (typically CN=7 or greater) and they tend to form complexes with “hard” fluoride and oxygen-donor ligands. Coordination numbers less than 6 are extremely rare in f -block coordination chemistry, and they were not observed for lanthanides until the three-coordinate tris[bis(trimethylsilyl) amide] complexes were synthesized in the 1970's [10-13]. These volatile, low-coordinate complexes with bulky silyl-amide ligands have led to important advances in the field [14-18].

They have served as gateways to new uncharted areas of f -block coordination chemistry via the “silyl-amide protonolysis route” [15, 19-23]; for example, the tris[bis(trimethylsilyl)amides] of the lanthanides have been used to install anionic, “soft-donor” sulfido [20,21], selenido [21], tellurido [22], and phosphido [19] ligands via protonolysis. The volatility of lanthanide and actinide tris(silyl)amides makes them naturally attractive for metal-organic chemical vapor deposition (MOCVD) applications. The sulfido (thiolate) complexes have been used as precursors for the synthesis of high-purity lanthanide sulfide (Ln_2S_3) materials [2]. The tris-silylamides themselves can be used for the synthesis of lanthanide nitride (LnN) materials [15,24, 25], and uranium tris-amides can also be used to make uranium nitride (UN) [26], which has been attracting a lot of attention as a next generation nuclear fuel [26]. Nitride fuels have several advantages, such as high thermal conductivity, thermal stability, and fissile metal



Figure 1: Sublimed $U[N(SiMe_3)_2]_3$



Scheme 1: General Synthesis of $\text{M}_f^{\text{III}} [\text{OPR}_3][\text{N}(\text{SiMe}_3)_2]_3$

density; however, the synthesis of high purity actinide nitrides has been proven very difficult using conventional carbothermic reduction methods from metal oxides [26]. Molecular actinide amide precursors provide a potential alternative for the synthesis of high purity actinide nitride fuels [26].

$\text{Gd}[\text{N}(\text{SiMe}_3)_2]_3$ and $\text{Nd}[\text{N}(\text{SiMe}_3)_2]_3$ have recently been used as single-source precursors for the synthesis of bimetallic MRI contrast agents (Gd) [27] and efficient photoabsorbers (Nd) [28], respectively. $\text{U}[\text{N}(\text{SiMe}_3)_2]_3$ and $\text{Er}[\text{N}(\text{SiMe}_3)_2]_3$ exhibit slow magnetic relaxation and are single-ion magnets [29,30]. *f*-Element single-ion magnets, and their potential applications in quantum technologies, has been the subject of a few excellent review articles in recent years [30-33]. $\text{Ce}[\text{N}(\text{SiMe}_3)_2]_3$ (Figure 1a) has served as a gateway for the synthesis of four-coordinate Cerium(IV) halide complexes [34-38]. These new tetravalent Cerium halide compounds represent an important advance in Ce^{IV} chemistry [38] and provide a high-symmetry platform for investigating the uranium-like covalency that has recently been observed in Ce^{IV} metal-ligand bonding [8]. Tris(silyl)amides have also provided straightforward and reliable routes to low-coordinate tetravalent uranium [39,40] and plutonium [24,25] halide compounds, as well as tetravalent, pentavalent, and hexavalent

uranium complexes with metal-ligand multiple bonds [33-38]. Indeed, it is an exciting time to be involved in *f*-element coordination chemistry.

Over the decades since $\text{Ln}[\text{N}(\text{SiMe}_3)_2]_3$ compounds were first synthesized, they have also been used to synthesize four-coordinate trivalent adducts with Lewis-bases, such as triphenylphosphine oxide [49-51]. The triphenylphosphine oxide adducts have exhibited interesting reactivity. In a previous study, the four-coordinate triphenylphosphine oxide adducts showed enhanced protonolysis reactivity with diphenylphosphine (HPPH_2) compared to the base-free three-coordinate $\text{Ln}[\text{N}(\text{SiMe}_3)_2]_3$ compounds [19]. These protonolysis reactions resulted in the synthesis of lanthanum, europium, and yttrium phosphido complexes. Very few lanthanide complexes with anionic phosphorus-donor ligands have been reported in the literature [2,19,52,53]. This observed enhancement in reactivity has yet to be further explored since it was first reported decades ago, and it is worth revisiting and investigating further. The pseudo- C_3 symmetric four-coordinate tris[bis(trimethylsilyl)amido] triphenylphosphine oxide framework has only been reported for La [19], Sm [51], Eu [19], Er [50], Lu [19], Y [19], and U [39]. Only the lanthanum and uranium derivatives that have been characterized by X-ray crystallography

[19,39], and ^{31}P NMR spectra have only been reported for the diamagnetic derivatives (La and Y) [19]. To our knowledge, tris(silylamido) phosphine oxide complexes with *substituted-aryl* phosphine oxide ligands have not been characterized via XRD or NMR. Substituted aryl-derivatives exhibit different reactivities and spectroscopic properties than the simple triphenylphosphine oxide framework, because the relative electron density on the phosphorus and oxygen atoms is highly influenced by the electronic character of the organic substituents bound to the phosphorus. The nature of the organic substituents on phosphorus therefore

highly influences the nature of the metal-oxygen bond in phosphine oxide coordination complexes.

These axially symmetric four-coordinate silyl-amide phosphine oxide complexes are suitable models for studying the relative differences in Ln/An metal-ligand covalency using ^{31}P -NMR spectroscopy and X-ray emission spectroscopy. Expanding this structural framework to other lanthanide and actinide metals, and fully characterizing a series of *pseudo-isomorphous* complexes featuring various organic substituents on the phosphine

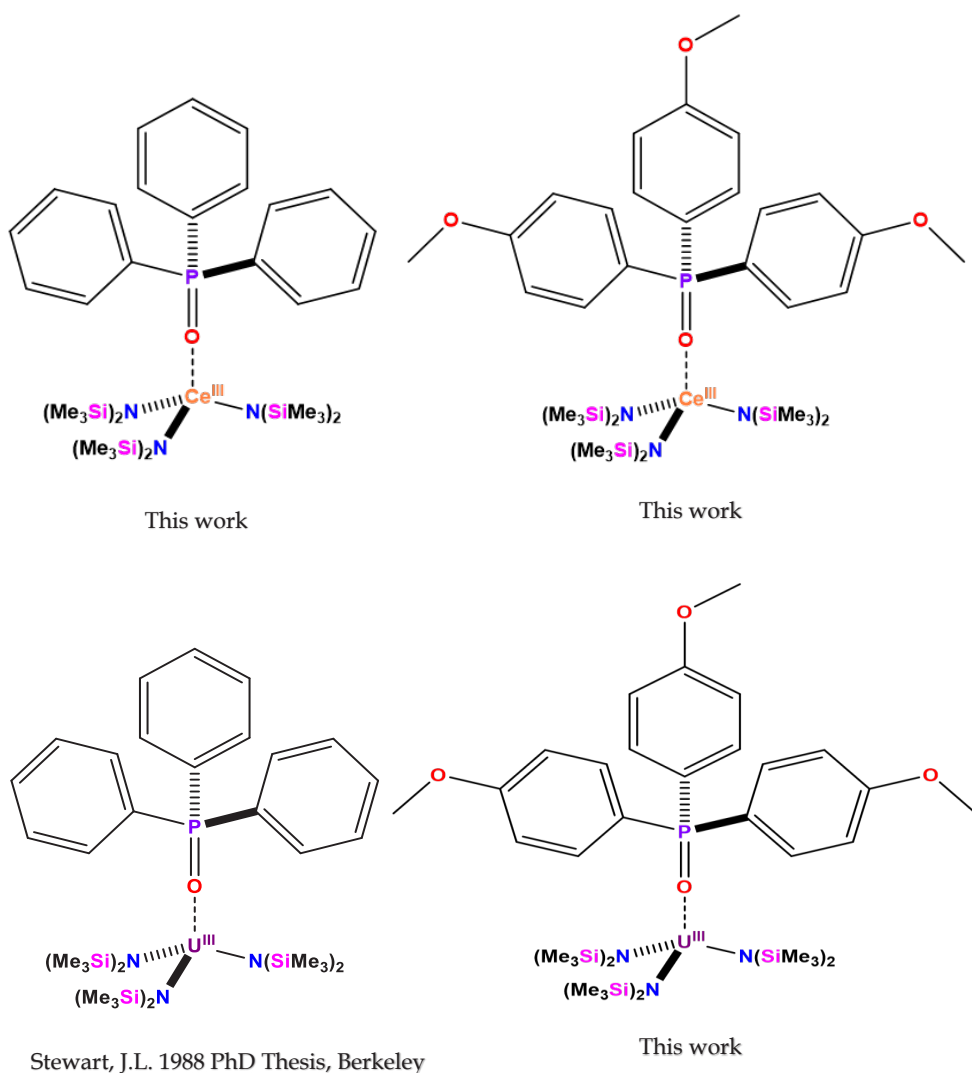


Figure 2: Structurally Characterized $\text{M}_f^{\text{III}}[\text{OPAr}_3][\text{N}(\text{SiMe}_3)_2]_3$ Compounds

oxide (beyond triphenylphosphine oxide), would provide considerable insight concerning phosphine oxide bonding interactions with *f*-block metals. In addition to being convenient ligands for spectroscopic studies of *f*-element electronic structure, phosphine oxides (and the details of their interactions with *f*-block metals) are directly relevant to the nuclear fuel cycle [54]. Phosphine oxides have been used effectively for advanced trivalent lanthanide/actinide separations [54-56]. The fundamental nature of *f*-block metal-phosphine oxide bonds is not well understood [7,57,58,59], and deeper empirical insight into the nature of these interactions is needed in order to facilitate large-scale computational screening of potential extractants for trivalent Ln/An separations.

Herein we report the synthesis, X-ray crystallography, and paramagnetic NMR spectroscopy of a series of trivalent cerium and uranium tris(silylamido) phosphine oxide complexes, as well as the X-ray and gamma emission spectra for Ce[N(SiMe₃)₂]₃[OPPh₃].

Experimental

All experimental operations were conducted with rigorous exclusion of air and moisture using Schlenk techniques, standard glove-box methods using a Vacuum Atmospheres glovebox with a recirculating dinitrogen atmosphere, and standard glove-bag methods using a Captair Pyramid disposable glove-box under Argon. Solvents were bought anhydrous or HPLC grade (pentane, hexane, toluene, acetonitrile, THF, diethyl ether) and further purified using a Vacuum Atmospheres Solvent Purifier System. 1,4-dioxane, THF, and diethyl ether were dried over sodium benzophenone ketyl, and degassed by three freeze-pump-thaw cycles prior to use. All solvents were stored under dinitrogen in a glove-box, and stored over 4 Å molecular sieves for at least 24 hours prior to use. Glassware was dried at 150°C before use. ¹H and ³¹P NMR spectra were recorded using a Bruker 400 MHz spectrometer at 298 K. Deuterated benzene (Cambridge Isotopes) was stored over 4 Å molecular sieves for at least 24 hours prior to use. Elemental analysis was conducted using particle-

induced X-ray emission spectrometry (PIXE) and particle-induced gamma-ray emission spectrometry (PIGE) using a 3 MeV proton beam generated by a 3MV Tandem Accelerator (National Electrostatics Corporation). X-rays were detected using two high-energy Bruker SDD detectors, and one low-energy Bruker SDD detector. Gamma-rays were detected using a liquid nitrogen-cooled high-purity germanium (HPGe) detector. The sample for elemental analysis was secured between two pieces of 8 μm Kapton film under nitrogen and brought out into the atmosphere for external ion beam analysis. Single crystal X-ray diffraction was conducted using a Bruker XRD instrument with a Mo-Kα X-ray source.

Oxide encrustations were removed from the uranium metal using concentrated nitric acid [60]. Once the turnings achieved a brilliant lustre, the nitric acid was decanted, and the turnings were rinsed with acetone and stored in a dinitrogen atmosphere glovebox. Iodine (sublimed) was used as purchased (Aldrich). KN(SiMe₃)₂ and CeCl₃ (anhydrous) was used as purchased (Aldrich). Phosphine oxides were synthesized from commercially obtained tertiary-arylphosphines (Aldrich) using literature methods [61, 62]. U₃(1,4-dioxane)_{1,5} was prepared using literature methods [60]. Ce[N(SiMe₃)₂]₃ [63] and U[N(SiMe₃)₂]₃ [60] were synthesized using literature methods and sublimed prior to use.

Caution! Depleted uranium (primary isotope ²³⁸U) is a weak α-emitter (4.197 MeV) with a half-life of 4.47 x 10⁹ years; manipulations and reactions should be carried out in monitored fume hoods or in an inert atmosphere drybox in a radiation laboratory equipped with α- and β-counting equipment.

Synthesis of Ce[OPPh₃]₃[N(SiMe₃)₂]₃

0.739 grams (1.19 mmol) of freshly sublimed Ce[N(SiMe₃)₂]₃ was dissolved in 10 mL of toluene, and added to a flask with 0.331 grams (1.19 mmol) of triphenylphosphine oxide, and stirred overnight at room temperature. The vibrant yellow color of the Ce[N(SiMe₃)₂]₃ slowly fades to transparent as the triphenylphosphine oxide

coordinates to the Cerium ion. The solvent was removed *in-vacuo*, and the residue was extracted with 20 mL of pentane, and filtered through a Celite-padded, medium porosity fritted-filter. The pentane was removed from the product *in vacuo*, and a beige-tan solid was afforded in 87% yield (0.928 grams). Large crystals were grown from a concentrated pentane solution with a minimal amount of toluene. The crystals initially submitted were twinned, and the product was recrystallized from a pentane/toluene solution to yield a large (ca. 0.5 g) crystal with smaller single crystals surrounding it. The smaller crystals were submitted for single crystal X-ray diffraction, and the crystal structure obtained confirmed that the compound was indeed the four-coordinate complex tris(silyl) amide phosphine oxide complex. The proton NMR for the complex features a large, broad, paramagnetically shifted SiMe_3 peak at -0.78 ppm, which is relatively more deshielded than the three-coordinate precursor (-3.3 ppm). Very broad aromatic NMR signals also show up at 6.4 ppm and 4.6 ppm, relatively more shielded compared to the free ligand. The observation of only two aromatic signals is consistent with the isostructural Yttrium complex [49]. Only one ^{31}P NMR resonance was observed at 54

ppm, significantly deshielded compared to the free ligand at 29 ppm. The large crystal was submitted for ion beam analysis, and the X-ray spectrum obtained via PIXE nearly confirms the correct stoichiometry of the complex. The relative Ce and Si concentrations were almost correct; however, the P concentrations were somewhat high, presumably due to the phosphine oxide crust that formed on the crystal over time. *Crystal Data*: $\text{C}_{36}\text{H}_{69}\text{CeN}_3\text{OPSi}_6$ (1-Ce), $M = 899.57$, triclinic, space group , $a = 12.3341(10) \text{ \AA}$, $b = 12.3809(10) \text{ \AA}$, $c = 19.7051(17) \text{ \AA}$, $\alpha = 100.0905(13)^\circ$, $\beta = 93.0661(14)^\circ$, $\gamma = 118.9017(12)^\circ$, $U = 2560.0(4) \text{ \AA}^3$, $Z = 2$, $D = 1.167 \text{ g cm}^{-3}$, Mo-K α radiation [$\lambda = 0.71073 \text{ \AA}$, $\mu(\text{Mo-K}\alpha) = 1.087 \text{ mm}^{-1}$]. *NMR Data* (C_6D_6): ^1H δ -0.78 ppm (SiMe_3 , 54H), δ 6.4 ppm (aromatic 9H), δ 4.6 ppm (aromatic 6H); ^{31}P δ 53.57 ppm. *Elemental Analysis* (PIXE): Calculated Ce 15.58 P 3.44 Si 18.73; Found: Ce 15.58 P 6.48 Si 19.67.

Synthesis of $\text{Ce}[\text{OP}(p\text{-anisyl})_3][\text{N}(\text{SiMe}_3)_2]_3$

0.021 grams (0.034 mmol) of freshly sublimed $\text{Ce}[\text{N}(\text{SiMe}_3)_2]_3$ was dissolved in 3 mL of toluene, and added to a flask with 0.012 grams (0.034 mmol) of tris(*p*-anisyl) phosphine oxide, and stirred overnight at room

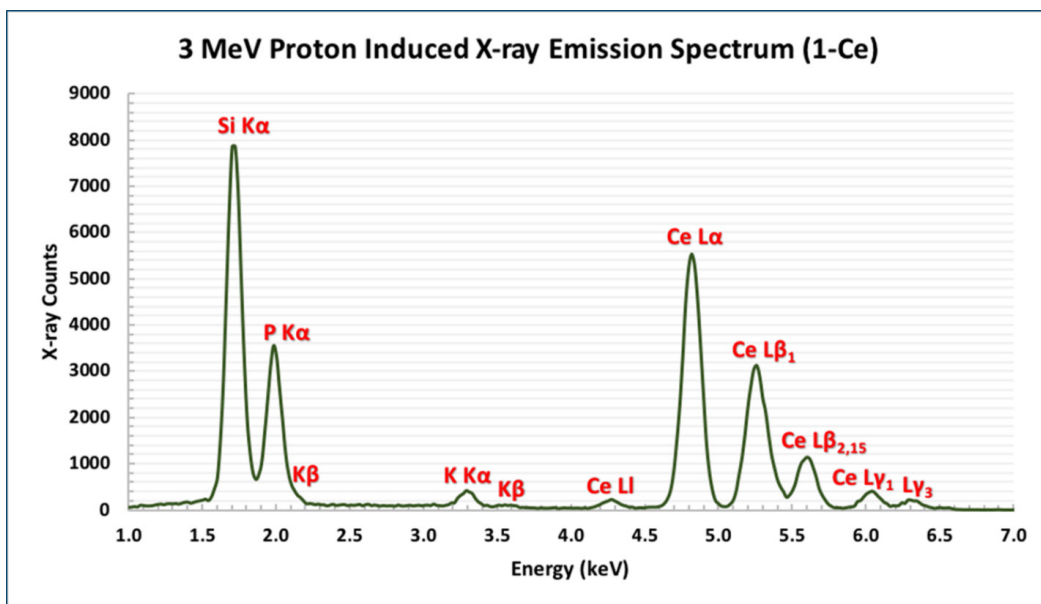


Figure 3: Energy-Dispersive X-ray Emission Spectrum for $\text{Ce}[\text{OPPh}_3][\text{N}(\text{SiMe}_3)_2]_3$

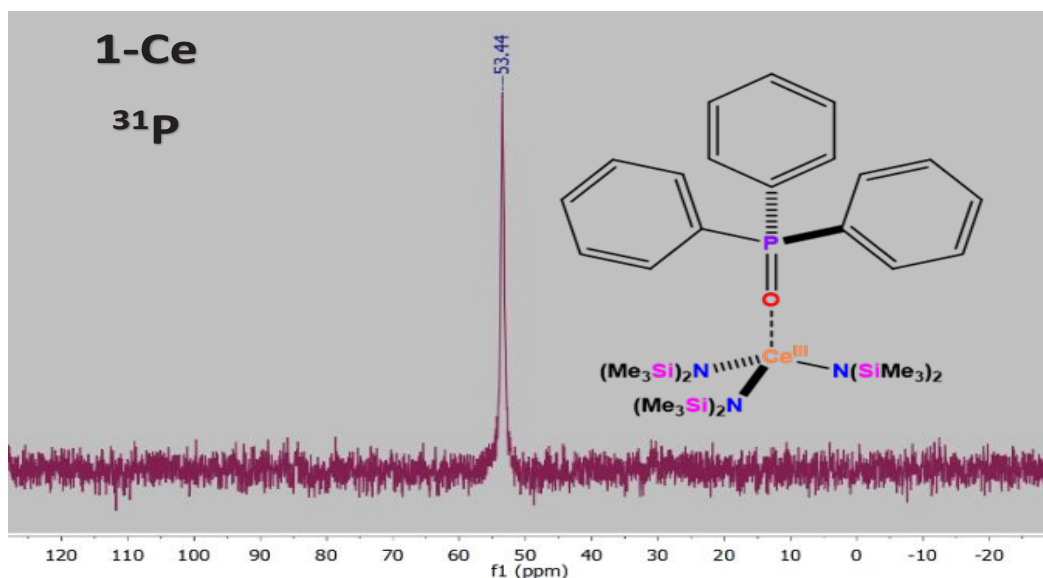


Figure 4: ³¹P NMR Spectrum for Ce[OPPh₃][N(SiMe₃)₂]₃

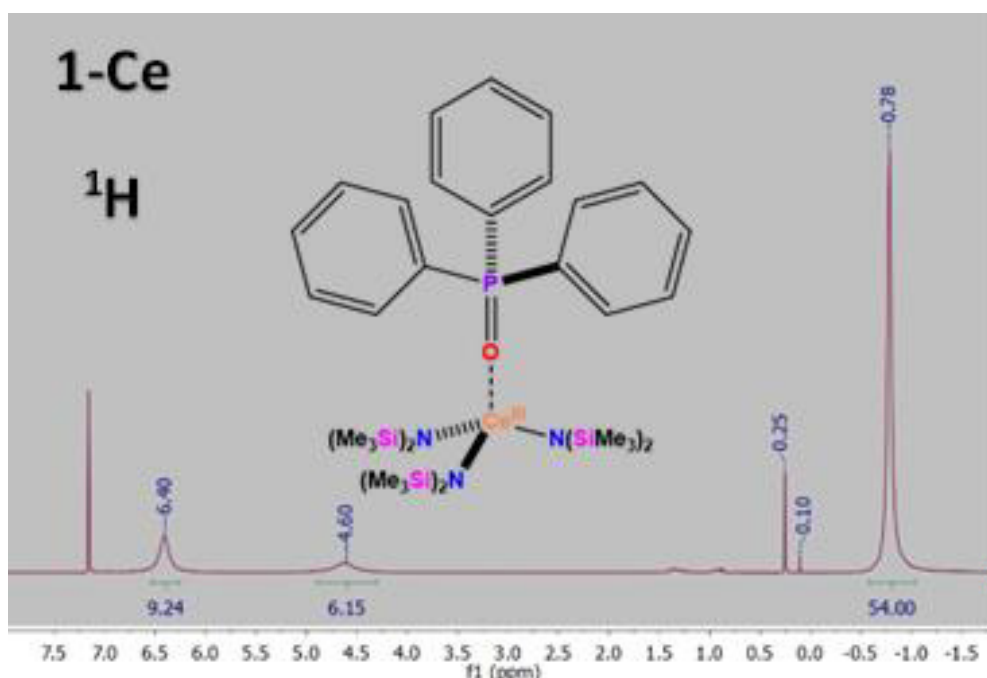


Figure 5: ¹H NMR Spectrum for Ce[OPPh₃][N(SiMe₃)₂]₃

temperature. The vibrant yellow color of the Ce[N(SiMe₃)₂]₃ slowly fades to transparent as the tris(*p*-anisyl)phosphine oxide coordinates to the cerium ion. The solvent was removed *in vacuo*, and the residue was extracted with 10 mL of pentane, and filtered through a Celite-

padded, medium porosity fritted-filter. The pentane was removed from the product *in vacuo*, and a colorless solid was afforded in ca. 100% yield (0.033 grams). Single crystals were grown from a concentrated pentane solution via slow evaporation at room temperature after a few

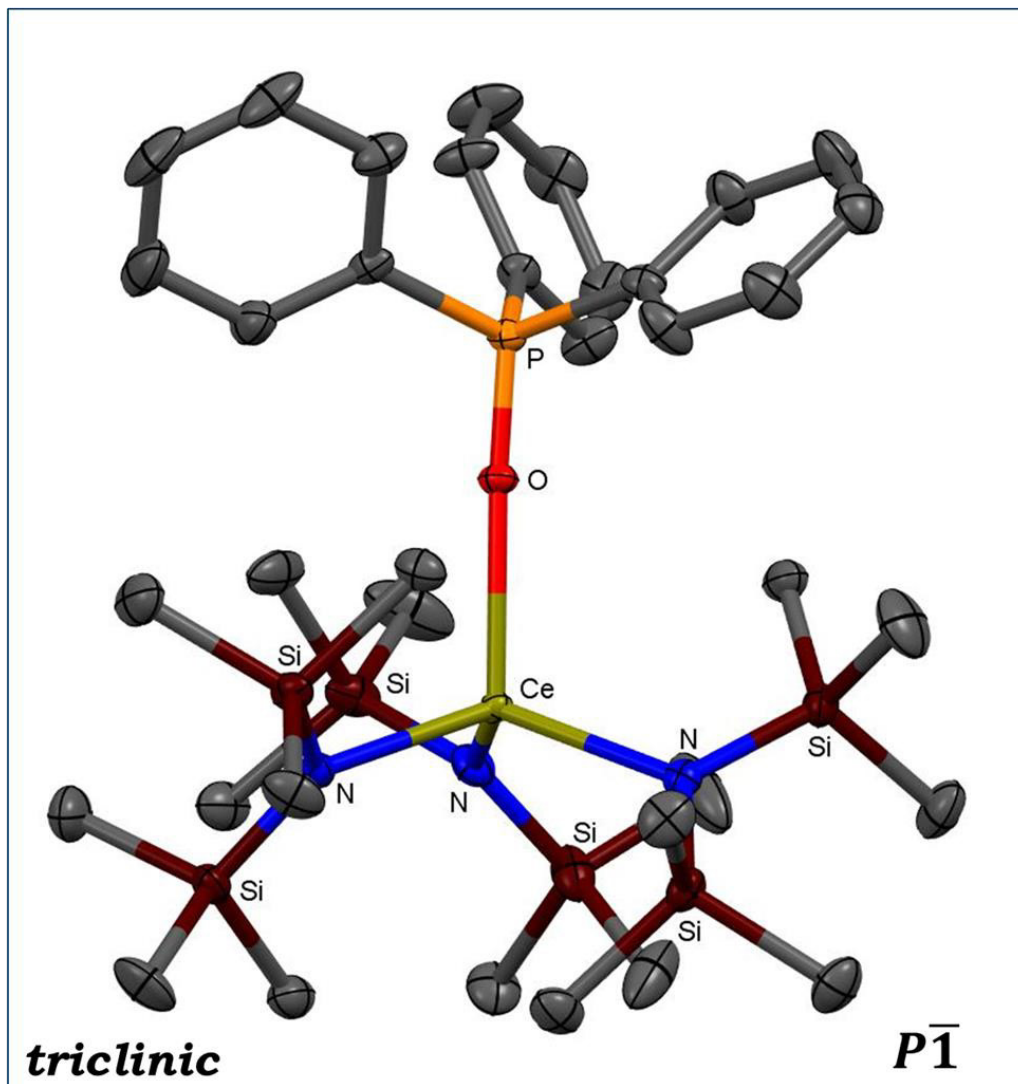


Figure 6: Single-Crystal XRD Structure for $Ce[OPPh_3][N(SiMe_3)_2]_3$

days and submitted for X-ray diffraction. *Crystal Data*: $C_{39}H_{75}CeN_3O_4PSi_6$ (2-Ce), $M = 989.65$, monoclinic, space group $P2_1/c$, $a = 16.1035(9)$ Å, $b = 13.8776(8)$ Å, $c = 23.0565(13)$ Å, $\alpha = 90^\circ$, $\beta = 91.9766(9)^\circ$, $\gamma = 90^\circ$, $U = 5149.6(5)$ Å³, $Z = 4$, $D_c = 1.276$ g cm⁻³, Mo-K α radiation [$\lambda = 0.71073$ Å, $\mu(\text{Mo-K}\alpha) = 1.092$ mm⁻¹]. *NMR Data* (C_6D_6): 1H δ -0.77 ppm (SiMe₃, 54H), δ 6.14 ppm (aromatic 6H), δ 4.92 ppm (aromatic 6H), δ 2.98 ppm (OCH₃, 9H); ^{31}P δ 54.39 ppm.

Synthesis of $U[OP(p\text{-anisyl})_3][N(SiMe_3)_2]_3$

0.719 grams (1.03 mmol) of freshly sublimed

$U[N(SiMe_3)_2]_3$ was dissolved in 10 mL of toluene, and added to a flask with 0.379 grams (1.03 mmol) of tris(*p*-anisyl)phosphine oxide, and stirred overnight at room temperature. The reddish-purple color of the $U[N(SiMe_3)_2]_3$ appears to gradually change to a darker shade of purple very subtly as the tris(*p*-anisyl)phosphine oxide coordinates to the uranium ion. The solvent was removed *in-vacuo*, and the residue was extracted with 20 mL of pentane, and filtered through a Celite-padded, medium porosity fritted-filter. The pentane was removed from the product *in vacuo*, and a purple solid

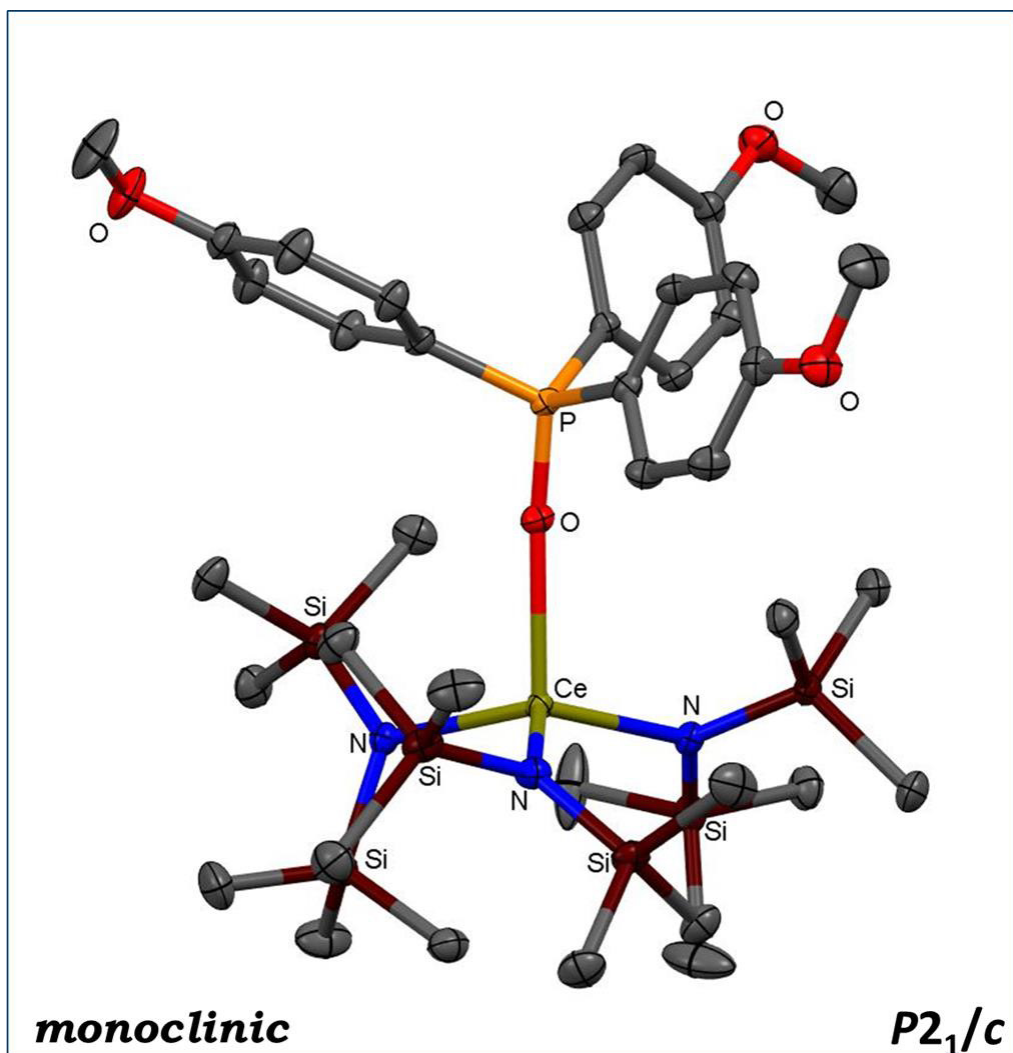
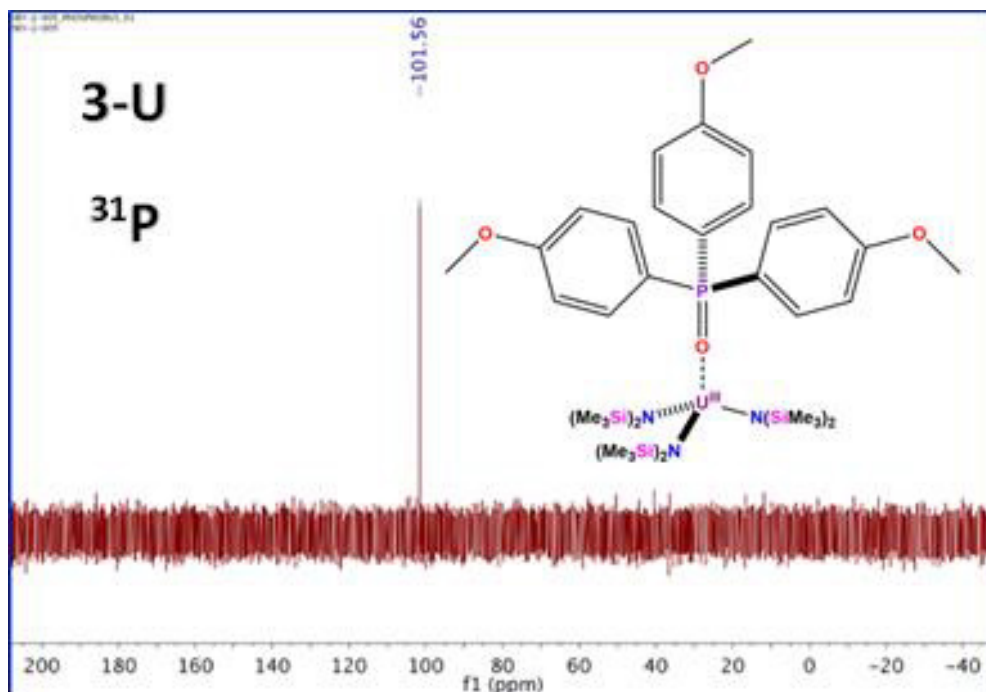
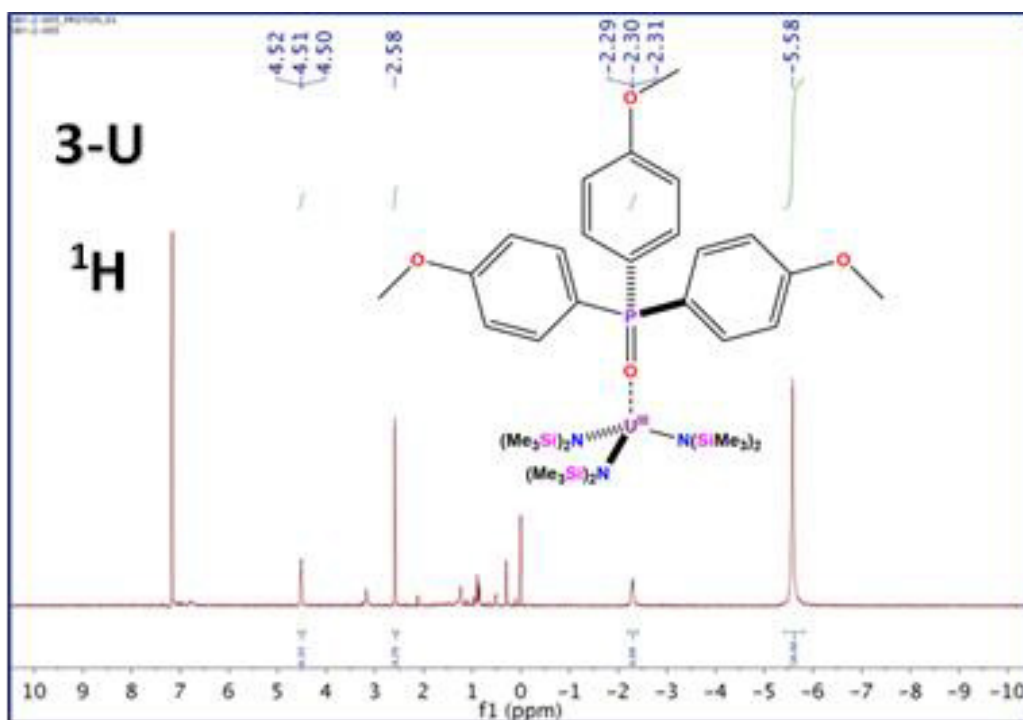


Figure 7: Single-Crystal XRD Structure for $\text{Ce}[\text{OP}(p\text{-anisyl})_3][\text{N}(\text{SiMe}_3)_2]_3$

was afforded in 46% yield (0.519 grams).

Alternative procedure 0.051 grams (0.068 mmol) of $\text{U}_3(1,4\text{-dioxane})_{1.5}$ was dissolved in 5 mL of THF. Three equivalents of $\text{KN}(\text{SiMe}_3)_2$ and a threefold excess of *t* tris(*p*-anisyl)phosphine oxide (with respect to uranium) was dissolved in 5 mL of THF, and added dropwise to the U_3/THF solution while stirring at room temperature with slight evolution of fumes upon addition. The dark brown (almost black) solution was stirred overnight, and the solvent was removed *in vacuo*. The residue was extracted with toluene, and the potassium iodide salts were removed by filtering the extract through a Celite-padded

medium porosity fritted filter. The solvent was removed *in vacuo* yielding a dark-brown/black solid, and the residue was extracted with *n*-pentane. The remaining salts and unidentified insoluble by-products were removed by filtering the purple *n*-pentane extract through a Celite-padded medium-porosity fritted filter. The solvent was removed *in vacuo*, affording a purple solid in ca 50% yield. Purple single-crystals of the complex were grown from a concentrated pentane solution via slow evaporation at -30°C after a few days and submitted for X-ray diffraction. *Crystal Data:* $\text{C}_{39}\text{H}_{75}\text{N}_3\text{O}_4\text{PSi}_6\text{U}$ (3-U), $M = 1087.56$, monoclinic, space group $P2_1/c$, $a = 16.063(2) \text{ \AA}$, $b = 13.9300(19) \text{ \AA}$, c

Figure 8: ^{31}P NMR Spectrum for $\text{U}[\text{OP}(p\text{-anisyl})_3][\text{N}(\text{SiMe}_3)_2]_3$ Figure 9: ^1H NMR Spectrum for $\text{U}[\text{OP}(p\text{-anisyl})_3][\text{N}(\text{SiMe}_3)_2]_3$

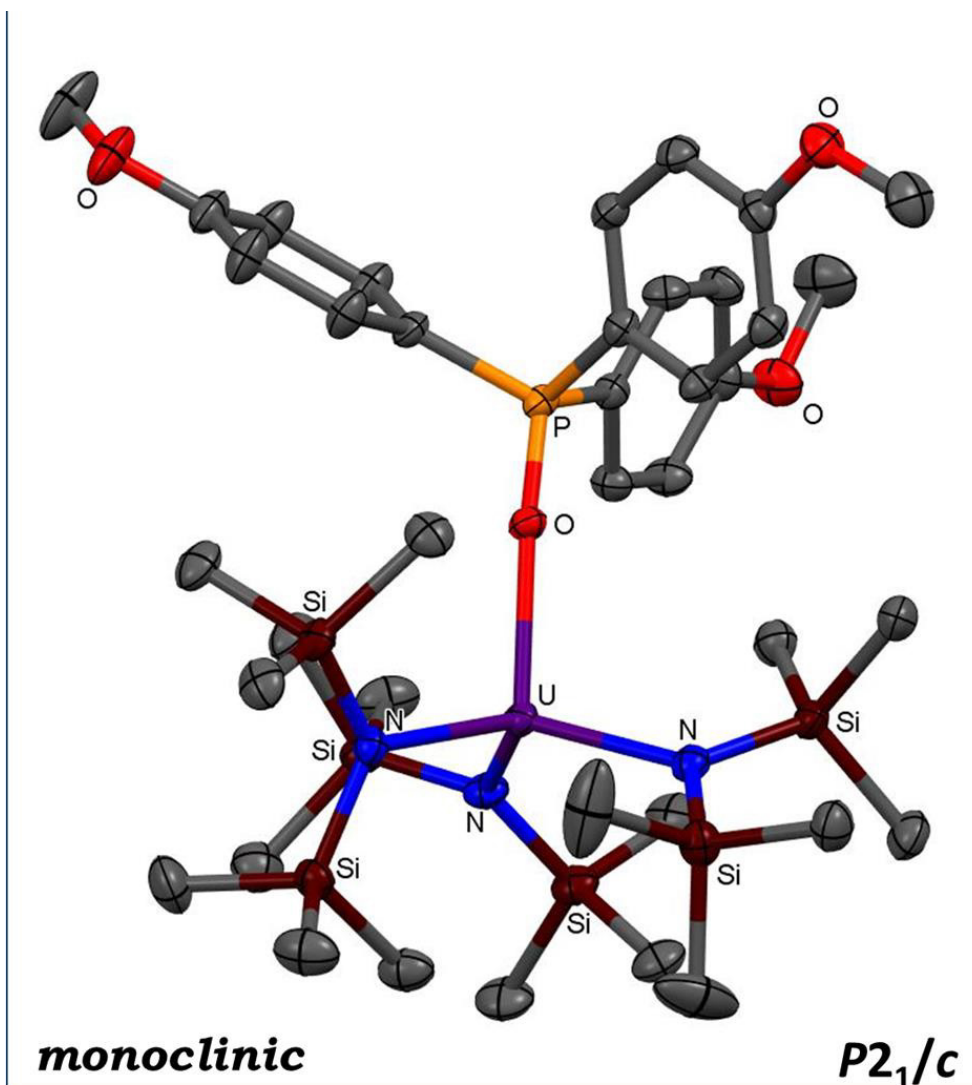


Figure 10: Single-Crystal XRD Structure for $U[OP(p\text{-anisyl})_3][N(SiMe_3)_2]_3$

$a = 23.043(3) \text{ \AA}$, $\alpha = 90^\circ$, $\beta = 91.895(2)^\circ$, $\gamma = 90^\circ$, $U = 5153.2(12) \text{ \AA}^3$, $Z = 4$, $D_c = 1.402 \text{ g cm}^{-3}$, Mo-K α radiation [$\lambda = 0.71073 \text{ \AA}$, $\mu(\text{Mo-K}\alpha) = 3.357 \text{ mm}^{-1}$]. *NMR Data* (C_6D_6): 1H δ -5.68 ppm ($SiMe_3$, 54H), δ 4.47 ppm (aromatic 6H), δ -2.51 ppm (aromatic 6H), δ 2.56 ppm (OCH_3 , 9H); ^{31}P δ 102.6 ppm.

Synthesis of $Ce[OP(p\text{-tolyl})_3][N(SiMe_3)_2]_3$

0.009 grams (0.0148 mmol) of freshly sublimed $Ce[N(SiMe_3)_2]_3$ was dissolved in 3 mL of toluene, and added to a flask with 0.005 grams (0.0148 mmol) of tris(*p*-tolyl)phosphine oxide,

and stirred overnight at room temperature. The vibrant yellow color of the $Ce[N(SiMe_3)_2]_3$ slowly fades to transparent as the tris(*p*-tolyl)phosphine oxide coordinates to the cerium ion. The solvent was removed *in vacuo*, and the residue was extracted with 10 mL of pentane, and filtered through a Celite-padded, medium porosity fritted-filter. The pentane was removed from the product *in vacuo*, and a beige solid was afforded in 52 % yield (0.007 grams). *NMR Data* (C_6D_6): 1H δ -0.74 ppm ($SiMe_3$, 54H), δ 5.45 ppm (aromatic 9H), δ 4.67 ppm (aromatic 6H); ^{31}P δ 54.55 ppm.

Table 1. Crystallographic Data for $R_3P=O-Met-[N(SiMe_3)_2]_3$

R	Met	bond length (Å)							bond angle (°)					ref
		Met-O	O-P	Met-N1	Met-N2	Met-N3	M-N _{avg}	Met-O=P	N1-Met-N2	N1-Met-N3	N2-Met-N3	N-Met-N _{avg}		
MeOPh	Ce	2.3952(12)	1.5161(12)	2.3612(14)	2.4000(14)	2.4065(14)	2.389	174.44(7)	107.37(5)	114.43(5)	121.53(5)	114.44		
Ph	Ce	2.403(2)	1.512(2)	2.357(2)	2.373(3)	2.388(2)	2.373	176.85(13)	108.83(9)	110.90(9)	116.96(9)	112.23		
MeOPh	U	2.376(3)	1.519(3)	2.344(4)	2.390(4)	2.398(4)	2.377	174.2(2)	108.55(14)	112.84(14)	120.88(14)	114.09		
Ph	U	2.382(2)	1.512(2)	2.343(4)	2.362(4)	2.367(3)	2.357	176.5(2)	109.8(1)	110.7(1)	115.6(1)	112.03	[26]	
Ph	La	2.40(2)	1.52(2)	2.38(2)	2.40(3)	2.41(2)	2.397	174.6	109.2(9)	112.7(8)	116.4(6)	112.77	[49]	

Table 2. Data for $Ph_3P=O-Met-[N(SiMe_3)_2]_3$ NMR data (ppm)

Met	³¹ P	¹ H SiMe ₃	¹ H Aromatic	ref
U	105.19	-5.66	6.46-4.56	
Ce	53.57	-0.78	6.40, 4.63	
La	39	0.07	7.57	[49]
Y	38	0.3	6.8-7.9	[49]
Sm	N/A	N/A	N/A	[51]
Eu	N/A	-1.43	4.9	[49]
Er	N/A	N/A	N/A	[50]
Lu	N/A	0.1	7.5	[49]

Results and Discussion

Reactions of extremely air sensitive $Ce[N(SiMe_3)_2]_3$ (CeN^*) and $U[N(SiMe_3)_2]_3$ (UN^*) with one equivalent of aryl-phosphine oxide ligands in toluene at room temperature for several hours afforded $M[OPAr_3][N^*]_3$ compounds in moderate to excellent yields (46%-100%). Optimum yields were obtained for the *para*-methoxy substituted aryl-phosphine oxide derivative (quantitative), and in general, cerium derivatives were obtained in better yields than the uranium derivatives. $U[OP(p-anisyl)]_3[N(SiMe_3)_2]_3$ could also be obtained in one step from directly $UI_3(1,4-dioxane)_{1.5}$, thereby circumventing the difficulties involved with obtaining impurity-free $U[N(SiMe_3)_2]_3$. The four-coordinate aryl-phosphine oxide adducts, unsurprisingly, are more air-stable and robust than their three-coordinate tris-amide precursors; however, the phosphine oxide adducts are still extremely air/moisture-sensitive, just less so than the extremely coordinatively unsaturated three-coordinate precursors. These aryl-phosphine oxide adducts are highly crystalline, and large single-crystals can be obtained via slow evaporation of *n*-pentane and/or toluene at

room temperature or $-30^\circ C$.

Single-crystal X-ray structures were obtained for $U[OP(p-anisyl)]_3[N(SiMe_3)_2]_3$, $Ce[OP(p-anisyl)]_3[N(SiMe_3)_2]_3$, and $Ce[OPPh_3][N(SiMe_3)_2]_3$, which facilitated useful comparisons with the two other structurally characterized tris(silyl)amido-triphenylphosphine oxide complexes reported in the literature, $La[OPPh_3][N(SiMe_3)_2]_3$ and $U[OPPh_3][N(SiMe_3)_2]_3$. These compounds also facilitated useful comparisons with the base-free tri-coordinate $M[N(SiMe_3)_2]_3$ complexes that have been structurally characterized [$M = Ce$ [64], Pr [65], Nd [66], Sm [67], Eu [68], Tb [69], Dy [70], Er [70], Tm [71], Yb [72], Lu [73], Y [74], Sc [68], U [75], and Pu [76)]. Additional comparisons can also be made with other *f*-element phosphine oxide complexes that have been structurally characterized [59]; however, to limit the scope of this discussion, attention will be focused on the extremely short list of monomeric four-coordinate tris[bis(trimethylsilyl)amido] Lewis-base adducts of the *f*-elements that have been structurally characterized. The three crystal structures obtained, along with the previously reported La and U derivatives, are *pseudo*-

isostructural, and feature nearly linear metal-oxygen-phosphorus bond angles (174-176°). Bond lengths and bond angles for this *pseudo*-isostructural series are given in Table 1. Table 4 gives the average metal-nitrogen bond lengths for the structurally characterized $M[N(\text{SiMe}_3)_2]_3$ derivatives for comparison.

The XRD data obtained in this work, in conjunction with previous XRD results, indicate that coordination of an aryl-phosphine oxide ligand to the tris(silyl)amido framework results in a subtle, but noticeable, lengthening of the metal-nitrogen bonds compared to the three-coordinate base-free analogues. The cerium-nitrogen bond in CeN^*_3 (2.320 Å) increases to 2.403 Å in $\text{Ce}[\text{OPPh}_3][\text{N}(\text{SiMe}_3)_2]_3$ and 2.395 Å in 2-Ce. The uranium-nitrogen bond in UN^*_3 (2.320 Å) increases to 2.382 Å in $\text{U}[\text{OPPh}_3][\text{N}(\text{SiMe}_3)_2]_3$ and 2.376 Å in 3-U. The metal-oxygen-phosphorus (M-O-P) bond angles are nearly linear in all the complexes. The M-O-P angles for the triphenylphosphine oxide complexes $\text{Ce}[\text{OPPh}_3][\text{N}(\text{SiMe}_3)_2]_3$ and $\text{U}[\text{OPPh}_3][\text{N}(\text{SiMe}_3)_2]_3$ are ca. 176°, and 174° for $\text{Ce}[\text{OP}(p\text{-anisyl})_3][\text{N}(\text{SiMe}_3)_2]_3$, $\text{U}[\text{OP}(p\text{-anisyl})_3][\text{N}(\text{SiMe}_3)_2]_3$, and $\text{La}[\text{OPPh}_3][\text{N}(\text{SiMe}_3)_2]_3$. The three triphenylphosphine oxide complexes have N-M-N angles of about 112° (average), and the angles for the substituted aryl derivatives are slightly larger, 114° (average). As a whole, the geometrical

parameters are extremely similar for the five tris(silyl)amido-phosphine oxide complexes that have been structurally characterized by XRD in this work and previous work.

The data in Table 4 shows a gradual decrease in lanthanide-nitrogen bond distances across the *4f* series from Ce-Yb as the relative ionic radius of the lanthanide ion decreases. The metal-nitrogen bond lengths in $\text{Ce}[\text{N}(\text{SiMe}_3)_2]_3$ and $\text{U}[\text{N}(\text{SiMe}_3)_2]_3$ are identical (2.320 Å), which is consistent with their nearly identical trivalent ionic radii. Since the ionic radii of La^{3+} (117.2 pm), Ce^{3+} (115 pm), and U^{3+} (116 pm) [2] are so similar, one might expect there to be little to no difference in the metal-oxygen bond lengths shown in Table 1. However, the uranium-oxygen bonds are measurably shorter than the cerium and lanthanum bonds. The differences in bond lengths are very subtle (only about 0.02 Å); however, this could be evidence of increased metal-ligand covalency in the uranium complexes compared to the cerium and lanthanum analogues, presumably due to slightly increased ligand *2p* orbital mixing into *6d* and *7p* manifolds. However, very little can be said definitively about the orbital interactions involved based on this slight difference in bond length.

The bonding in these *f*-element amide complexes is largely ionic in character, and most

Table 3. Data for $R_3\text{P}=\text{O}\text{-Met-}[\text{N}(\text{SiMe}_3)_2]_3$ NMR data (ppm)

R	Met	^{31}P	$^1\text{H SiMe}_3$	$^1\text{H Aromatic}$	$^1\text{H Alkyl}$	ref
<i>t</i> -Bu	Ce	91.77	-1.17	-	-5.14	
MePh	Ce	54.55	-0.74	5.45, 4.67	1.56	
MeOPh	Ce	54.39	-0.77	6.14, 4.92	2.98	
Ph	Ce	53.57	-0.78	6.40, 4.63	-	
MePh	U	98.34	-5.53	6.25, 4.63	-7.22	
<i>t</i> -Bu	U	368.58	-3.16	-	-8.75	
MeOPh	U	102.6	-5.68	4.47, -2.51	2.56	
$\text{Ph}_2(\text{tolyl})$	U	104.48	-5.52	6.85-4.51	-2.83	
Ph	U	105.19	-5.66	6.46-4.56	-	
Ph	La	39	0.07	7.57	-	[49]

Table 4. $M_r^{III}[N(SiMe_3)_2]_3$

$Ln^{III}[N(SiMe_3)_2]_3$	1H NMR	ref	Ln-N Bond	ref
La	0.25	[10]		
Ce	-3.39	[63]	2.320(3)	[64]
Pr	-8.64	[10]	2.31(4)	[65]
Nd	-6.25	[63]	2.29(4)	[66]
Sm	-1.58	[10]	2.284(3)	[67]
Eu	6.43	[10]	2.259(9)	[68]
Gd	-11.07	[63]		
Tb			2.233(12)	[69]
Dy			2.212(2)	[70]
Ho				
Er	62.89	[63]	2.21(1)	[70]
Tm			2.198(9)	[71]
Yb			2.158(13)	[72]
Lu	0.1	[10]	2.168(12)	[73]
Y	0.28	[10]	2.224(6)	[74]
Sc			2.047(6)	[68]
$An^{III}[N(SiMe_3)_2]_3$				
U	-11	[14]	2.320(4)	[75]
Np	3.01	[14]		
Pu	0.74	[14]	2.315(10)	[76]

of the structural data can be rationalized in terms of the ionic radius of the central metal cation, and the steric properties of the ligand framework. However, the relative amount of metal-ligand covalency in lanthanide amide complexes appears to have been initially underestimated, with the assumption that the limited radial extent of the core-like $4f$ orbitals prevented nitrogen-metal π -interactions, leading to negligible metal-ligand covalency. Photoelectron studies seemed to confirm this assertion [77]. However, subsequent computational studies suggested that lanthanide amides have a considerable degree of covalent character. While affirming the conclusions of previous studies with respect to the non-involvement of the $4f$ electrons in chemical bonding, some computational results emphasize the importance of the $5d$ and $6p$ orbitals in lanthanide-nitrogen bonds [93].

Empirical structural and spectroscopic data for lanthanide amide and phosphine oxide complexes are scarce, and more isostructural complexes of the other members of the lanthanide series and actinide series need to be synthesized and characterized. Sophisticated computational and spectroscopic studies must also be conducted on these complexes before any real conclusions about the nature of the metal-ligand bonds in these complexes can be made. This work is a small step in that direction.

Paramagnetic 1H and ^{31}P NMR spectra were obtained for $Ce[OP(p\text{-anisyl})_3][N(SiMe_3)_2]_3$, $Ce[OPPh_3][N(SiMe_3)_2]_3$, and $U[OP(p\text{-anisyl})_3][N(SiMe_3)_2]_3$, along with other substituted aryl- and alkyl-derivatives. Derivatives other than $Ce[OP(p\text{-anisyl})_3][N(SiMe_3)_2]_3$, $Ce[OPPh_3][N(SiMe_3)_2]_3$, and $U[OP(p\text{-anisyl})_3][N(SiMe_3)_2]_3$

have not yet been fully characterized or obtained in pure form; however, tentative assignments for additional aryl and alkyl derivatives could still be made for the paramagnetically shifted NMR resonances that were observed, so they are included here for comparison. Table 2 features the NMR data for Ce[OPPh₃][N(SiMe₃)₂]₃, as well as all the NMR data available in the literature for M[OPPh₃][N(SiMe₃)₂]₃ complexes. Table 3 features the NMR data for Ce[OP(*p*-anisyl)₃][N(SiMe₃)₂]₃, Ce[OPPh₃][N(SiMe₃)₂]₃, and U[OP(*p*-anisyl)₃][N(SiMe₃)₂]₃, along with additional data for complexes that have not been fully characterized or obtained in pure form. Tables 2 and 3 also include NMR data for the previously reported U[OPPh₃][N(SiMe₃)₂]₃. No NMR data was previously reported for this complex, though its crystal structure was reported in Stewart's 1988 dissertation. Synthetic difficulties were encountered in this work while trying to reproduce the U[OPPh₃][N(SiMe₃)₂]₃ complex, similar to the difficulties Stewart reported in her 1988 dissertation. Presumably the instability of the complex is what prevented the NMR data from being acquired. Stewart reported that the purple solid complex decomposed to a brown microcrystalline solid after prolonged exposure to vacuum. In our hands, the characteristic purple color of the complex persisted for a short time while in an inert-atmosphere glove-box; however, by the time the compound was worked-up, isolated, and analyzed by NMR, the purple color had turned to brown, and complex NMR spectra were obtained that were difficult to assign. However, synthesis of U[OPPh₃][N(SiMe₃)₂]₃ directly from UI₃(1,4-dioxane)_{1.5} (described in the experimental section for the alternative synthesis U[OP(*p*-anisyl)₃][N(SiMe₃)₂]₃), yielded NMR spectra that could be assigned with a relatively high degree of confidence. One of the more interesting results of this work is that the *para*-methoxy-substituted aryl-phosphine oxide complex, U[OP(*p*-anisyl)₃][N(SiMe₃)₂]₃, seems to be more stable than U[N(SiMe₃)₂]₃[OPPh₃]. U[OP(*p*-anisyl)₃][N(SiMe₃)₂]₃ repeatedly gave clear, easily assignable NMR spectra. The alternative route directly from UI₃(1,4-dioxane)_{1.5} gave cleaner, reproducible results for the synthesis of U[OP(*p*-anisyl)₃][N(SiMe₃)₂]₃

and the other aryl- and alkyl-substituted phosphine oxide complexes shown in Table 3.

The NMR spectra obtained for Ce[OP(*p*-anisyl)₃][N(SiMe₃)₂]₃, Ce[OPPh₃][N(SiMe₃)₂]₃, and U[OP(*p*-anisyl)₃][N(SiMe₃)₂]₃, and other less characterized systems, exhibited large paramagnetic shifts in both the ¹H and ³¹P NMR spectra. The paramagnetic shifts for the uranium complexes were much larger than the cerium complexes, which is consistent with the fact that uranium has more unpaired *f*-electrons with an *f*⁸ configuration compared to cerium with an *f*¹ configuration. The pseudocontact contribution is the primary influence on the NMR spectra of *f*-elements [2,10,49,78,79], and the large shifts caused by the interactions between unpaired *f*-electrons and ligand nuclei in Ce[OP(*p*-anisyl)₃][N(SiMe₃)₂]₃, Ce[OPPh₃][N(SiMe₃)₂]₃, and U[OP(*p*-anisyl)₃][N(SiMe₃)₂]₃ are mainly dipolar in origin [2,80]. *f*-electrons are very localized and core-like, and do not tend to delocalize onto ligand atoms to a large extent. *f*-electron interactions with ligand nuclei are “through-space” interactions [2,80]. These “through-space” interactions require the *f*-metal ion to have an anisotropic distribution of *f*-electrons [81]. The following equation predicts the relative variation in dipolar shifts for the lanthanide series (assuming axial symmetry):

$$\delta^{pcs} = \frac{-\mu_0 g_l^2 \mu_B^2 J(J+1)(2J-1)(2J+3)}{4\pi} \frac{D_z(3\cos^2\theta - 1)}{60(kT)^2 r^3}$$

where

$$g_l = 1 + \frac{J(J+1) - L(L+1) + S(S+1)}{2J(J+1)}$$

Cerium(III) has a ²F_{5/2} ground state [2,81]; therefore, the Landé factor (*g_l*) is equal to 6/7. Uranium(III) has a ⁴I_{9/2} ground state [2,82], with a Landé factor (*g_l*) equal to 8/11. In some rare cases, when suitable delocalization mechanisms are involved, a small covalent contribution to metal-ligand bonding in *f*-element systems can occur. As a result, a “contact” shift can occur due to delocalization of unpaired *f*-electron density onto the ligand atoms [2,80,81]. The

mechanism of the spin density delocalization is due to weak covalent bonding involving the 6s orbital, which in turn can transfer unpaired spin density onto ligand nuclei via spin polarization from 4f orbitals [81].

NMR studies of $\text{Ln}[\text{N}(\text{SiMe}_3)_2]_3$ and $\text{Ln}[\text{N}(\text{SiMe}_3)_2]_3[\text{OPPh}_3]$ demonstrate the predominance of the pseudo-contact contribution to the paramagnetic shifts in this series [10,49]; however, some of the data suggest that a contact contribution is involved, and there is considerable evidence that lanthanide amides have significant contact contributions to their paramagnetic shifts [10,49]. Separating the pseudocontact and contact contributions for the shifts observed for $\text{Ce}[\text{OP}(p\text{-anisyl})_3]_3[\text{N}(\text{SiMe}_3)_2]_3$, $\text{Ce}[\text{OPPh}_3]_3[\text{N}(\text{SiMe}_3)_2]_3$, and $\text{U}[\text{OP}(p\text{-anisyl})_3]_3[\text{N}(\text{SiMe}_3)_2]_3$ is beyond the scope of this discussion, and is the subject of future work using Density Functional Theory (DFT) and Quantum Theory of Atoms in Molecules (QTAIM). QTAIM has recently been used to analyze the paramagnetic NMR shifts of actinide complexes in order to estimate relative metal-ligand covalency via the QTAIM *delocalization index* [83].

The X-ray emission spectrum for $\text{Ce}[\text{OPPh}_3]_3[\text{N}(\text{SiMe}_3)_2]_3$ (obtained using a low-energy SDD detector) is shown in Figure 4.3. The characteristic X-ray lines for cerium, phosphorus,

and silicon are present, and concentrations obtained from the Ce $L\alpha$ (4.84 keV), P $K\alpha$ (2.015 keV), and Si $K\alpha$ (1.739 keV) peaks are close to the predict values (Calculated: Ce 15.58 P 3.44 Si 18.73; Found: Ce 15.58 P 6.48 Si 19.67). The relative cerium/silicon ratio is almost correct, but the relative phosphorus concentration is a little high (presumably due to the formation of a phosphine oxide crust on the crystal and sample decomposition over time). Potassium is also present in trace amounts (6578 ppm, 0.65 wt. %) due to the presence of unremoved KCl or unreacted $\text{K}(\text{SiMe}_3)_2$. This result shows that multiple sublimations are indeed necessary to remove the potassium salts, as has been done by some researchers [77]. The cerium $K\alpha$ peak was also observed at 34.717 keV in the high-energy X-ray emission spectrum with very low statistics.

In addition to the cerium $L\alpha_1$ X-ray emission, the $L\beta_1$, $L\beta_{2,15}$, $L\gamma_1$, $L\text{I}$ emissions were also observed (Figures 4.3 and 4.12). The 4.84 keV $L\alpha_1$ X-ray emission is a $M_5 \rightarrow L_3$, ($3d_{5/2} \rightarrow 2p_{3/2}$) electronic transition. The 4.3 keV $L\text{I}$ X-ray emission is a $M_1 \rightarrow L_3$ ($3s_{1/2} \rightarrow 2p_{3/2}$) electronic transition. The 5.262 keV $L\beta_1$ X-ray emission is a $M_4 \rightarrow L_2$ ($3d_{3/2} \rightarrow 2p_{1/2}$) electronic transition. The $L\beta_2$ and $L\beta_{15}$ X-ray emissions at ca. 5.7 keV are $N_5 \rightarrow L_3$ and $N_4 \rightarrow L_3$ ($4d_{5/2} \rightarrow 2p_{3/2}$ and $4d_{3/2} \rightarrow 2p_{3/2}$) electronic transitions, respectively. The

Table 5. ^{31}P NMR Chemical Shifts for $\text{M}[\text{N}(\text{SiMe}_3)_2]_3[\text{OPR}_3]$ NMR data (ppm)

f^n	M	R	$\text{M}[\text{N}(\text{SiMe}_3)_2]_3[\text{OPR}_3]$	$[\text{OPR}_3]$	$\Delta\delta$	ref
f^1	Ce	<i>t</i> -Bu	91.77	41	50.77	
f^1	Ce	MePh	54.55	29.88	24.67	
f^1	Ce	MeOPh	54.39	29.3	25.09	
f^1	Ce	Ph	53.57	29.65	23.92	
f^3	U	<i>t</i> -Bu	368.58	41	327.6	
f^3	U	MePh	98.34	29.88	68.46	
f^3	U	MeOPh	102.6	29.3	73.3	
f^3	U	$\text{Ph}_2(\text{tolyl})$	104.48	27.71	76.77	
f^3	U	Ph	105.19	29.65	75.54	
f^0	La	Ph	39	29.65	9.35	[49]

Table 6. ^1H NMR Chemical Shifts (SiMe_3 - ^{54}H) NMR data (ppm)

f^n	M	R	M[N(SiMe ₃) ₂] ₃ [OPR ₃]	Free M[N(SiMe ₃) ₂] ₃	$\Delta\delta$	ref
f^1	Ce	<i>t</i> -Bu	-1.17	-3.39	2.22	
f^1	Ce	MePh	-0.74	-3.39	2.65	
f^1	Ce	MeOPh	-0.77	-3.39	2.62	
f^1	Ce	Ph	-0.78	-3.39	2.61	
f^3	U	<i>t</i> -Bu	-3.16	-11	7.84	
f^3	U	MePh	-5.53	-11	5.47	
f^3	U	MeOPh	-5.68	-11	5.32	
f^3	U	Ph ₂ (tolyl)	-5.52	-11	5.48	
f^3	U	Ph	-5.66	-11	5.34	
f^0	La	Ph	0.7	0.25	-0.45	[10,49]
f^0	Y	Ph	0.3	0.28	-0.02	[10,49]
f^{14}	Lu	Ph	0.1	0.3	0.2	[10,49]
f^6	Eu	Ph	-1.43	6.43	-7.86	[10,49]

6.1 keV $L\gamma_1$ X-ray emission is a $N_4 \rightarrow L_2$ ($4d_{3/2} \rightarrow 2p_{1/2}$) electronic transition. The 6.33 keV $L\gamma_3$ X-ray emission is a $N_3 \rightarrow L_1$ ($4p_{3/2} \rightarrow 2s_{1/2}$) electronic transition. The 6.53 keV $L\gamma_4$ X-ray emission is a $O_3 \rightarrow L_1$ ($5p_{3/2} \rightarrow 2s_{1/2}$) electronic transition. A fair degree of fine structure can also be seen in the $L\gamma$ emissions. TD-DFT calculations could potentially be used to analyze the fine structure observed. The L emission series of cerium is sensitive to the chemical state of the complex, especially the higher energy transitions. It has recently been shown that the L emission energies and intensity ratios in energy-dispersive X-ray emission spectra vary depending on the chemical environment of rare-earth cations [84,85]. Comparison of the L emissions for a variety of Ce^{III} and Ce^{IV} compounds should be the subject of future work.

In addition to the silicon and phosphorus $K\alpha$ X-ray emissions peaks ($L_{2,3} \rightarrow K$ or $2p \rightarrow 1s$ transitions), the phosphorus $K\beta$ emission was also observed (Figure 4.13), albeit with very low statistics. The phosphorus $K\beta_1$ X-ray emission is a $M_3 \rightarrow K$, or $3p_{3/2} \rightarrow 1s$, electronic transition. This transition is highly sensitive to the chemical environment of the phosphorus atom because it is a valence-to-core transition. However, high resolution wavelength-dispersive X-ray emission using a crystal monochromator is required in order to achieve high enough

resolution to carry out phosphorus $K\beta$ analysis. Recent studies have shown that small ion accelerators can be used to perform wavelength-dispersive phosphorus $K\beta$ X-ray emission spectroscopy (WD-PIXE) [89]. These studies demonstrated that WD-PIXE yields results comparable to those obtained from advanced synchrotron light sources [89]. Phosphorus X-ray emission studies from other groups over the past several decades [86-89] have motivated us to use WD-PIXE for phosphorus $K\beta$ analysis for a variety of lanthanide and actinide compounds with phosphorus-based ligands. The phosphorus $K\beta$ X-ray emission from phosphine oxides and other phosphorus-based ligands has the potential to provide great insight into the nature f -metal-ligand bonding, especially when combined with results from phosphorus-31 NMR spectroscopy. This XES/NMR approach can facilitate the investigation of both *orbital-energy near-degeneracy driven covalency*, and *symmetry-restricted overlap driven covalency* in lanthanide and actinide coordination complexes. This should be the subject of future work. Such studies could potentially reveal periodic trends in metal-ligand orbital mixing for the f -block elements.

The proton-induced gamma emission spectrum for $\text{Ce}[\text{OPPh}_3][\text{N}(\text{SiMe}_3)_2]_3$ is shown in Figure 4.14. The gamma-emission at 1266 keV

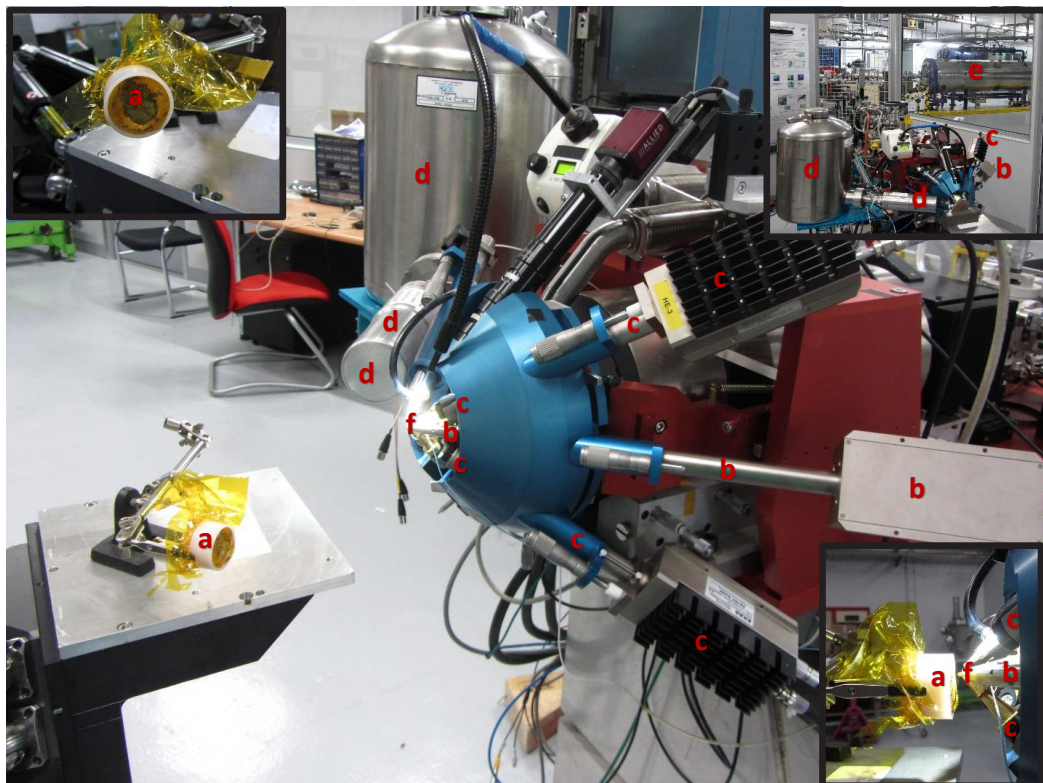


Figure 11: External Ion Beam Analysis setup at AGLAE, Louvre Museum, Paris, France. a) $\text{Ce}[\text{OPPh}_3][\text{N}(\text{SiMe}_3)_2]_3$ in sample holder, b) low-energy SDD X-ray detector, c) high-energy SDD X-ray detectors, d) HPGe Gamma detector, e) 3 MV Tandem Accelerator, f) 3 MeV proton beam exit window (Si_3N_4).

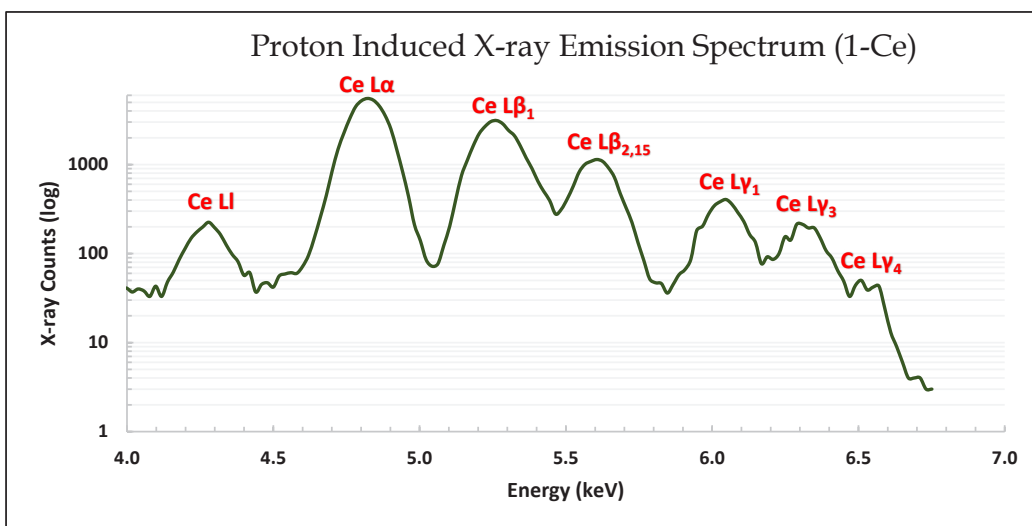


Figure 12: Cerium L X-ray Emission Series for $\text{Ce}[\text{OPPh}_3][\text{N}(\text{SiMe}_3)_2]_3$.

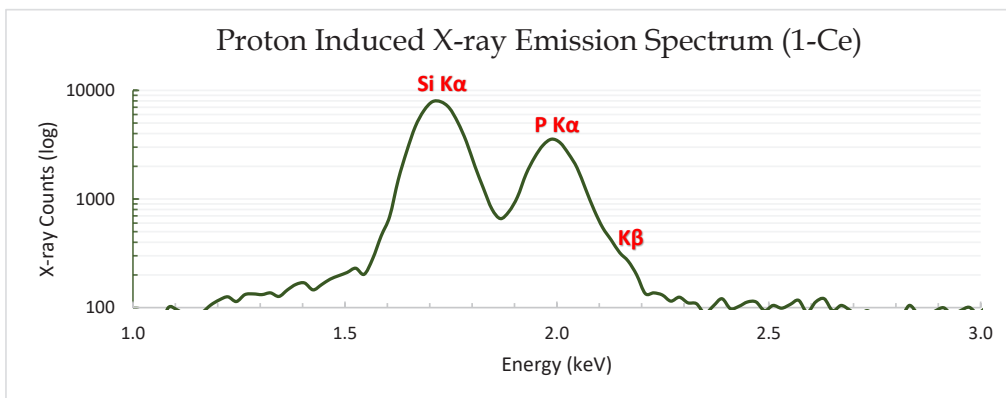


Figure 13: Silicon and Phosphorus K X-ray Emissions for $\text{Ce}[\text{OPPh}_3][\text{N}(\text{SiMe}_3)_2]_3$.

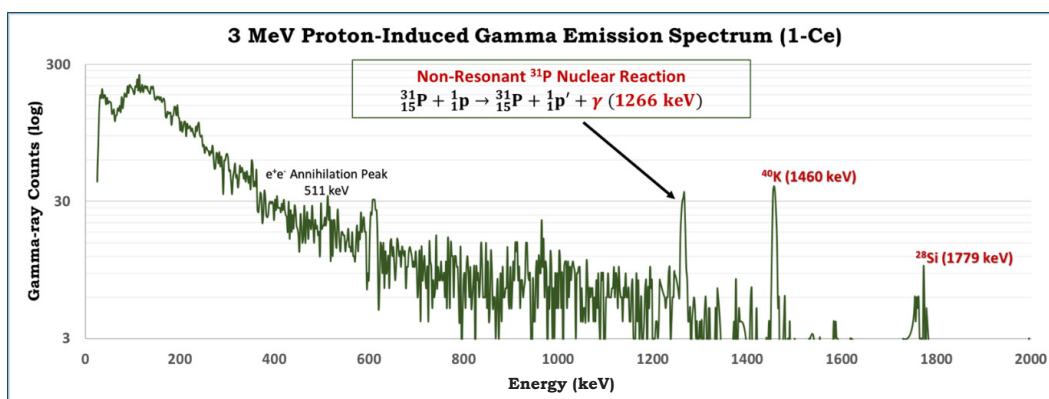


Figure 14: Proton-Induced Gamma Emission Spectrum for $\text{Ce}[\text{OPPh}_3][\text{N}(\text{SiMe}_3)_2]_3$.

corresponds to the non-resonant $^{31}\text{P}(p, p\gamma)^{31}\text{P}$ nuclear reaction. The e^+e^- annihilation peak was also observed at 511 keV. The observation of the emission resulting from the $^{31}\text{P}_{3/2} \rightarrow ^{31}\text{P}_{1/2}$ nuclear transition has inspired us to use this signal for nuclear electric field gradient studies *f*-metal complexes, similar to NQR (nuclear quadrupole resonance) electric field gradient studies that have been conducted on metal fluorides using time-differential perturbed angular distribution analysis (TD-PAD), which involves using an MeV proton beam to induce fluorine gamma-emission [90-92]. This should be the subject of future work.

Conclusion

Four-coordinate complexes of the lanthanides and actinides are extremely rare, and $\text{Ce}[\text{OP}(p\text{-anisyl})_3][\text{N}(\text{SiMe}_3)_2]_3$, $\text{Ce}[\text{OPPh}_3][\text{N}(\text{SiMe}_3)_2]_3$, and $\text{U}[\text{OP}(p\text{-anisyl})_3][\text{N}(\text{SiMe}_3)_2]_3$ are valuable contributions to *f*-element coordination chemistry. The X-ray crystal structures and paramagnetic NMR spectra for $\text{Ce}[\text{OP}(p\text{-anisyl})_3][\text{N}(\text{SiMe}_3)_2]_3$, $\text{Ce}[\text{OPPh}_3][\text{N}(\text{SiMe}_3)_2]_3$, and $\text{U}[\text{OP}(p\text{-anisyl})_3][\text{N}(\text{SiMe}_3)_2]_3$ are reported in this work, along with X-ray and gamma emission spectra for $\text{Ce}[\text{OPPh}_3][\text{N}(\text{SiMe}_3)_2]_3$. The results were presented in the context of data available from the previous literature, which allowed further insight into the nature of monomeric cerium(III) and uranium(III)

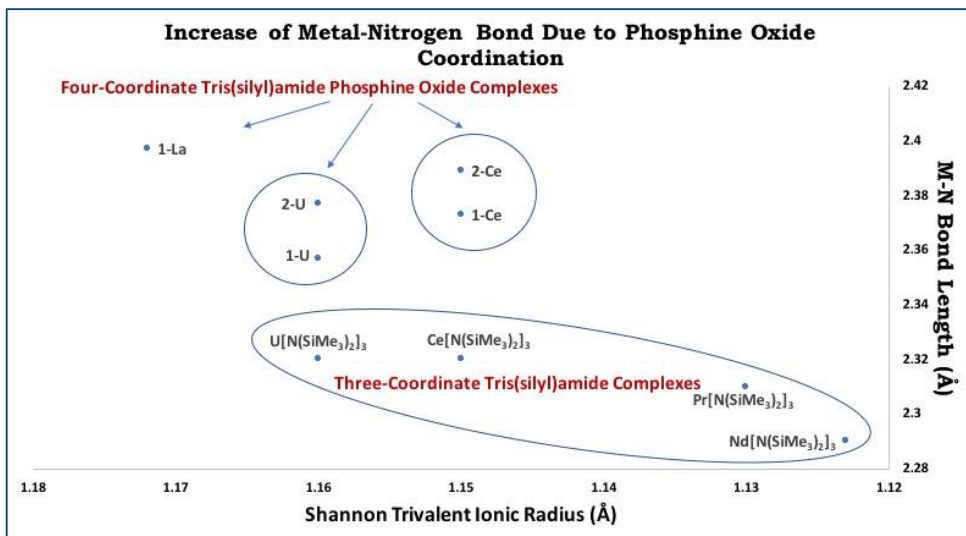


Figure 15: Increase in Metal-Nitrogen Bond Length with Phosphine Oxide Coordination

complexes with silylamide and phosphine oxide ligands. More insight will be achieved in future theoretical and experimental investigations of these model complexes. $\text{Ce}[\text{OP}(p\text{-anisyl})_3][\text{N}(\text{SiMe}_3)_2]_3$, $\text{Ce}[\text{OPPh}_2][\text{N}(\text{SiMe}_3)_2]_3$, and $\text{U}[\text{OP}(p\text{-anisyl})_3][\text{N}(\text{SiMe}_3)_2]_3$ can be used to investigate the previously observed enhancement in protonolysis reactivity of phosphine oxide adducts with diphenylphosphine (HPPH_2) compared to the base-free three-coordinate $\text{Ln}[\text{N}(\text{SiMe}_3)_2]_3$ compounds [19]. It was observed in this work that phosphine oxide coordination to the metal center increases the length of the metal-amide bond (see Figure 4.15), which could perhaps explain the enhanced protonolysis reactivity observed for similar rare-earth complexes decades ago [19].

Acknowledgements

The authors would like to thank the University of Oklahoma and the Department of Chemistry and Biochemistry for supporting this research. We would also like to thank Claire Pacheco, Thomas Calligaro, Quentin Lemasson, and Laurent Pichon for allowing the lead author to conduct external Ion Beam Analysis on 1-Ce at the AGLAE laboratory at C2RMF at the Louvre Museum in Paris, France. We would also like to thank Susan Nimmo at the University of Oklahoma NMR laboratory for her support and

assistance.

References

- [1] Kaltsoyannis, Nikolas and Peter Scott. 1999. *The f elements*. Oxford University Press, Oxford.
- [2] Aspinall, Helen C. 2001. *Chemistry of the f-Block Elements*. Gordon and Breach Science Publishers, Amsterdam.
- [3] Sastri, V.S., J.-C. Bünzli, V. Ramachandra Rao, G.V.S. Rayudu, and J.R. Perumareddi. 2003. *Modern Aspects of Rare Earths and their Complexes*. Elsevier, Amsterdam.
- [4] Cotton, Simon. 2006. *Lanthanide and Actinide Chemistry*. John Wiley & Sons, Ltd, Chichester.
- [5] Morss, Lester R., Norman M. Edelstein, Jean Fuger, Joseph J. Katz. *The Chemistry of the Actinide and Transactinide Elements*. Third edition. Springer, Dordrecht.
- [6] Atwood, David A. 2012. *The Rare Earth Elements: Fundamentals and Applications*. John Wiley & Sons, Ltd, Chichester.
- [7] Kaltsoyannis, Nikolas and Andrew Kerridge. 2014. "Chemical Bonding of Lanthanides and Actinides." In *The Chemical Bond: Chemical Bonding Across the Periodic Table*, pp.337-355, edited by Gernot Frenking and Sason Shaik. Wiley-VCH, Weinheim.

- [8] Kerridge, Andrew. 2017. "Quantification of f-element covalency through analysis of the electron density: insights from simulation." *Chemical Communication* 53: 6685-6695.
- [9] Dognon, Jean-Pierre. 2017. "Electronic structure theory to decipher the chemical bonding in actinide systems." *Coordination Chemistry Reviews* 344: 150-162.
- [10] Bradley, Donald C., Joginder S. Ghotra, and F. Alan Hart. "Low Co-ordination Numbers in Lanthanide and Actinide Compounds. Part I. The Preparation and Characterization of Tris{bis(trimethylsilyl)-amido}lanthanides." *Journal of the Chemical Society Dalton Transactions* 1973: 1021.
- [11] Ghotra, Joginder S., Michael B. Hursthouse, and Alan J. Welch. "Three-coordinate Scandium(III) and Europium(III); Crystal and Molecular Structures of their Tris-hexamethyl-disilylamides." 1973: 669.
- [12] Bradley, D.C. and J.S. Ghotra. 1975. "Mass Spectroscopic Studies on Metal Organosilylamides. Part I. Mass Spectra of Tris{bis(trimethylsilyl)amido}lanthanides." *Inorganica Chimica Acta* 13: 11-16.
- [13] Andersen, Richard A. 1979. "Tris((hexamethyl-disilyl)amido)uranium(III): Preparation and Coordination Chemistry." *Inorganic Chemistry* 18(6): 1507.
- [14] Avens, Larry R., Simon G. Bott, David L. Clark, Alfred Sattelberger, John G. Watkin, and Bill D. Zwick. 1994. "A Convenient Entry into Trivalent Actinide Chemistry: Synthesis and Characterization of $AnI_3(THF)_4$ and $An[N(SiMe_3)_2]_3$ ($An = U, Np, Pu$)." *Inorganic Chemistry* 33: 2248-2256.
- [15] Anwander, Reiner. 1996. "Lanthanide Amides." *Topics in Current Chemistry* 179: 33-112.
- [16] Drożdżyński, Janusz. 2005. "Tervalent uranium compounds." *Coordination Chemistry Reviews* 249: 2351-2373. University of Wrocław, Poland.
- [17] Baker, Robert J. 2012. "The coordination and organometallic chemistry of UI_3 and $U\{N(SiMe_3)_2\}_3$: Synthetic reagents par excellence." *Coordination Chemistry Reviews* 256: 2843-2871.
- [18] Emslie, David J. H. 2018. "Actinides: Amido Complexes." *Encyclopedia of Inorganic and Bioinorganic Chemistry*, John Wiley & Sons, Ltd., pp. 1-18.
- [19] Aspinall, Helen C., Donald C. Bradley, and Keith D. Sales. 1988. "Diphenylphosphido Complexes of the Lanthanides: Reactions of Compounds $[Ln\{N(SiMe_3)_2\}_3]$ ($Ln = La$ or Eu) or $[Ln\{N(SiMe_3)_2\}_3(Ph_3PO)]$ ($Ln = La, Eu, or Y$) with Ph_2PH to give $[Ln\{N(SiMe_3)_2\}_2(PPh_2)]$ or $[Ln\{N(SiMe_3)_2\}_2(PPh_2)(Ph_3PO)]$." *Journal of the Chemical Society Dalton Transactions*: 2211-2213.
- [20] Roger, Mathieu, Noémi Barros, Thérèse Arliguie, Pierre Thuéry, Laurent Maron, and Michel Ephritikhine. 2006. " $U(SMes^*)_n$ ($n = 3, 4$) and $Ln(SMes^*)_3$ ($Ln = La, Ce, Pr, Nd$): Lanthanide(III)/Actinide(III) Differentiation in Agostic Interactions and an Unprecedented η^3 Ligation Mode of the Arylthiolate Ligand, from X-ray Diffraction and DFT Analysis." *Journal of the American Chemical Society* 128: 8790-8802.
- [21] Aspinall, Helen C., Sharron A. Cunningham, Patirck Maestro, and Pierre Macaudierre. 1998. "Lanthanide Tris(*tert*-butylthiolates) and the Crystal Structure of $[Yb(SBu^t)_2(\mu_2-SBu^t)(Bipy)]_2$." *Inorganic Chemistry* 37: 5396-5398.
- [22] Cary, Douglas R. and John Arnold. 1993. "Preparation of Lanthanide Tellurolates and Evidence for the Formation of Cluster Intermediates in Their Thermal Decomposition to Bulk Metal Tellurides." *Journal of the American Chemical Society* 115: 2520-2521.
- [23] Gaunt, Andrew J., Sean D. Reilly, Alejandro E. Enriquez, Brian L. Scott, James A. Ibers, Permal Sekar, Kieran I.M. Ingram, Nikolas Kaltsoyannis, and Mary P. Neu. 2008. "Experimental and Theoretical Comparison of Actinide and Lanthanide Bonding in $M[N(EPR)_2]_3$ Complexes ($M = U, Pu, La, Ce$; $E = S, Se, Te$; $R = Ph, iPr, H$)." *Inorganic Chemistry* 47: 29-41.
- [24] LaDuca, Robert L. and Peter T. Wolczanski. 1992. "Preparation of Lanthanide Nitrides via Ammonolysis of Molten $\{(Me_3Si)_2N\}_3Ln$: Onset of Crystallization Catalyzed by $LiNH_2$ and $LiCl$." *Inorganic Chemistry* 31: 1311-1313.

- [25] Baxter, David V., Malcom H. Chrisholm, Gennaro J. Gama, and Vincent F. Distasi. 1996. "Molecular Routes to Metal Carbides, Nitrides, and Oxides. 2. Studies of the Ammonolysis of Metal Dialkylamides and Hexamethyldisilylamides." *Chemistry of Materials* 8: 1222-1228.
- [26] Czerwinski, K., and T. Hartmann. 2006. *Solution-Based Synthesis of Nitride Fuels*. UNLV, Fuels Campaign: Transmutation Research Program Projects.
- [27] Siribbal, Shifaa M., Johannes Schläfer, Shaista Liyas, Zhangjun Hu, Kajsa Uvdal, Martin Valldor, and Sanjay Mathur. 2018. "Air-Stable Gadolinium Precursors for the Facile Microwave-Assisted Synthesis of Gd_2O_3 Nanocontrast Agents for Magnetic Resonances Imaging." *Crystal Growth and Design* 18: 633-641.
- [28] Jamil, Aida, Johannes Schläfer, Yakup Gönüllü, Ashish Lepcha, and Sanjay Mathur. 2016. "Precursor-Derived Rare Earth Metal Pyrochlores: $Nd_2Sn_2O_7$ Nanofibers and Thin Films As Efficient Photoabsorbers." *Crystal Growth and Design* 16: 5260-5267.
- [29] Zhang, Peng, Li Zhang, Chao Wang, Shufang Xue, Shuang-Yan Lin, and Jinkui Tang. 2014. "Equatorially Coordinated Lanthanide Single Ion Magnets." *Journal of the American Chemical Society* 136: 4484-4487.
- [30] McAdams, Simon G., Ana-Maria Ariciu, Andreas K. Kostopoulos, James P.S. Walsh, and Floriana Tuna. 2017. "Molecular single-ion magnets based on lanthanides and actinides: Design considerations and new advances in the context of quantum technologies." *Coordination Chemistry Reviews* 346: 216-239.
- [31] Liddle, Stephen T. and Joris van Slageren. 2015. "Improving f-element single molecule magnets." *Chemical Society Reviews* 44: 6655-6669.
- [32] Meihaus, Katie R. and Jeffery R. Long. 2015. "Actinide-based single-molecule magnets." *Dalton Transactions* 44: 2517-2528.
- [33] a) Tang, J. and P Zhang. 2015. *Lanthanide Single Molecule Magnets*. Springer-Verlag, Berlin. b) Layfield, Richard A. and Muralee Murugesu. 2015. *Lanthanides and Actinides in Molecular Magnetism*. Wiley-VCH, Verlag.
- [34] Eisenstein, Odlie, Peter B. Hitchcock, Alexander G. Hulkes, Michael F. Lappert, and Laurent Maron. 2001. "Cerium masquerading as a Group 4 element: synthesis, structure and computational characterization of $[CeCl\{N(SiMe_3)_2\}_3]$." *Chemical Communications*: 1560-1561.
- [35] Dröse, Peter, Alan R. Crozier, Samira Lashkari, Jochen Gottfriedsen, Steffen Blaurock, Cristian G. Hrib, Cäcilla Maichle-Mössmer, Christoph Schädle, Reiner Anwander, and Frank T. Edlmann. 2010. "Facile Access to tetravalent Cerium Compounds: One-Electron Oxidation Using Iodine(III) Reagents." *Journal of the American Chemical Society Communication* 132: 14046-14047.
- [36] Williams, Ursula J., Jerome R. Robinson, Andrew J. Lewis, Patrick J. Carroll, Patrick J. Walsh, and Eric J. Schelter. 2014. "Synthesis, Bonding, and Reactivity of a Cerium(IV) Fluoride Complex." *Inorganic Chemistry* 53: 27-29.
- [37] Williams, Ursula J., Patrick J. Carroll, and Eric J. Schelter. 2014. "Synthesis and Analysis of a Family of Cerium(IV) Halide and Pseudohalide Compounds." *Inorganic Chemistry* 53: 6338-6345.
- [38] So, Yat-Ming and Wa-Hung Leung. 2017. "Recent advances in the coordination chemistry of cerium(IV) complexes." *Coordination Chemistry Reviews* 340: 172-197.
- [39] Stewart, Joanne Lee. 1988. *Tris[bis(trimethylsilyl)amido]uranium: Compounds with Tri-, Tetra-, and Penta-valent Uranium*. PhD Dissertation, University of California, Berkeley. Berkeley, California.
- [40] Thomson, R.K., C.R. Graves, B.L. Scott, and J.L. Kiplinger. 2011. "Straightforward and efficient oxidation of tris(aryloxide) and tris(amide) uranium(III) complexes using copper(I) halide reagents." *Inorganic Chemistry Communications* 14: 1742-1744.

- [41] Gaunt, Andrew J., Alejandro E. Enriquez, Sean D. Reilly, Brian L. Scott, and Mary P. Neu. 2008. "Structural Characterization of $\text{Pu}[\text{N}(\text{SiMe}_3)_2]_3$, a Synthetically Useful Nonaqueous Plutonium(III) Precursor." *Inorganic Chemistry* 47: 26-28.
- [42] Gaunt, Andrew J., Sean D. Reilly, Alejandro E. Enriquez, Trevor W. Hayton, James M. Boncella, Brian L. Scott, and Mary P. Neu. 2008. "Low Valent molecular Plutonium Halide Complexes." *Inorganic Chemistry* 47: 8412-8419.
- [43] Fortier, Skye, Jessie L. Brown, Nikolas Kaltsoyannis, Guang Wu, and Trevor Hayton. 2012. "Synthesis, Molecular, and Electronic Structure of $\text{U}^{\text{V}}(\text{O})[\text{N}(\text{SiMe}_3)_2]_3$." *Inorganic Chemistry* 51: 1625-1633.
- [34] Lewis, Andrew J., Eiko Nakamaru-Ogiso, James M. Kikkawa, Patrick J. Carroll, and Eric J. Schelter. 2012. "Pentavalent uranium *trans*-dihalides and -pseudohalides." *Chemical Communications* 48: 4977-4979.
- [35] Brown, Jessie L., Skye Fortier, Richard A. Lewis, Guang Wu, and Trevor W. Hayton. 2012. "A Complete Family of Terminal Uranium Chalcogenides, $[\text{U}(\text{N}\{\text{SiMe}_3\}_2)_3]^-$ (E = O, S, Se, Te)." *Journal of the American Chemical Society* 134: 15468-15475.
- [36] Smiles, Danil E., Guang Wu, and Trevor Hayton. 2014. "Synthesis of Uranium-Ligand Multiple Bonds by Cleavage of a Trityl Protecting Group." *Journal of the American Chemical Society* 136: 96-99.
- [37] Smiles, Danil E., Guang Wu, and Trevor Hayton. 2014. "Reversible Chalcogen-Atom Transfer to a Terminal Uranium Sulfide." *Inorganic Chemistry* 53: 12683-12685.
- [48] Smiles, Danil E., Guang Wu, and Trevor Hayton. 2014. "Synthesis of Terminal Monochalcogenide and Dichalcogenide Complexes of Uranium Using Polychalcogenides, $[\text{E}_n]^{2-}$ (E = Te, $n = 2$; E = Se, $n = 4$), as Chalcogen Atom Transfer Reagents." *Inorganic Chemistry* 53: 10240-10247.
- [49] Bradley, Donald C., Joginder S. Ghotra, F. Alan Hart, Michael B. Hursthouse, and Paul R. Raithby. 1977. "Low Co-ordination Numbers in Lanthanoid and Actinoid Compounds. Part 2. Syntheses, Properties, and Crystal and Molecular Structures of Triphenylphosphine Oxide and Peroxoderivatives of [Bis(trimethylsilyl-amido)]lanthanoids." *Journal of the Chemical Society Dalton Transactions*: 1166-1172.
- [50] Jank, Stefan, Clemens Guteenberger, Hauke Reddmann, Jan Hanss, and Hanns-Dieter Amberger. 2006. "Zur Elektronenstruktur hochsymmetrischer Verbindungen der f-Elemente. 41. Syntheses, Kristall-, Molekül- und Elektronenstruktur eines Bis(cyclohexylisnitrol)-Addukts des Grundkörpers Tris(bis(trimethylsilyl)amidoerbium(III) sowie Elektronenstrukturen ausgewählter Monoaddukte." *Zeitschrift für Anorganische und Allgemeine Chemie* 632: 2429-2438.
- [51] Jank, Stefan, Hauke Reddmann, Lixin Zhang, and Hanns-Dieter Amberger. 2012. "Zur Elektronenstruktur hochsymmetrischer Verbindungen der f-Elemente. 45. Ungewöhnliche spektrochemische Eigenschaften des Triphenylphosphinoxidoliganden im Falle von Mono- und Bisaddukten homoleptischer Samarium(III)silylamide." *Zeitschrift für Anorganische und Allgemeine Chemie* 638: 1159-1166.
- [52] Schumann, H. and G.M. Frisch. 1982. *Zeitschrift für Naturforschung, Teil B* 36: 1244.
- [53] Evans, W.J., I. Bloom, W.E. Hunter, and J.L. Atwood. 1983. *Organometallics* 2: 709.
- [54] Law, J.D., K.N. Brewer, R.S. Herbst, T.A. Todd, and D.J. Wood. 1999. "Development and demonstration of solvent extraction processes for the separation of radionuclides from acidic radioactive waste." *Waste Management* 19: 27-37.
- [55] Krahn, Elizabeth, Cécile Marie, and Kenneth Nash. 2016. Probing organic phase ligand exchange kinetics of 4f/5f solvent extraction systems with NMR spectroscopy. *Coordination Chemistry Reviews* 316: 21-35.

- [56] Romanovsky, V.N. 1998. *R&D Activities on Partitioning in Russia*. V.G. Khlopin Radium Institute, pp. 1-9.
- [57] Hällér, L.J.L., N. Kaltsoyannis, M.J. Sarsfield, L. May, S.M. Cornet, M.P. Redmond, and M. Helliwell. 2007. *Inorganic Chemistry* 46: 4868.
- [58] Platt, Andrew W.G. 2017. "Lanthanide phosphine oxide complexes." *Coordination Chemistry Reviews* 340: 62-78.
- [59] Lobana, T.S. 1992. "Coordination chemistry of phosphine chalcogenides and their analytical and catalytic applications." In *The Chemistry of Organophosphorus Compounds, Volume 2, Phosphine Oxides, Sulphides, Selenides, and Tellurides*, edited by Frank Hartley, pp. 409-566. John Wiley & Sons, Ltd.
- [60] Monreal, Marisa J., Robert K. Thomson, Thibault Cantat, Micholas E. Travia, Brian L. Scott, and Jaqueline L. Kiplinger. 2011. " $\text{UI}_4(1,4\text{-dioxane})_2$, $[\text{UCl}_4(1,4\text{-dioxane})]_2$, and $\text{UI}_3(1,4\text{-dioxane})_{1.5}$: Stable and Versatile Starting Materials for Low- and High-Valent Uranium Chemistry." *Organometallics* 30: 2031-2038
- [61] Woollins, J. Derek. 2010. *Inorganic Experiments. Third Edition*. Wiley-VCH, Weinheim.
- [62] Denton, Ross M., Jie An, Beatrice Adeniran, Alexander J. Blake, William Lewis, and Andrew Poulton. 2011. "Catalytic Phosphorus(V)-Mediated Nucleophilic Substitution Reactions: Development of a Catalytic Appel Reaction." *Journal of Organic Chemistry* 76: 6749-6767.
- [63] Edleman, Nikki L., Anchuan Wang, John A. Belot, Andrew W. Metz, Jason R. Babcock, Amber M. Kawaoka, Jun Ni, Matthew V. Metz, Christine J. Flashenriem, Charlotte L. Stern, Louise M. Liable-Sands, Arnold L. Rheingold, Paul R. Markworth, Robert P.H. Chang, Michael P. Chudzik, Carl R. Kannewurf, and Tobin J. Marks. 2002. "Synthesis and Characterization of Volatile, Fluorine-Free β -Ketoiminate Lanthanide MOCVD Precursors and Their Implementation in Low-Temperature Growth of Epitaxial CeO_2 Buffer Layers for Superconducting Electronics." *Inorganic Chemistry* 41: 5005-5023.
- [64] Rees, Jr., William S., Oliver Just, and Donald S. van Derveer. 1999. "Molecular design of dopant precursors for atomic layer epitaxy of SrS:Ce ." *Journal of Material Chemistry* 9: 249-252.
- [65] Fjeldberg, T., Andersen, R.A. 1985. *Journal of Molecular Structure* 129: 93.
- [66] Andersen, R.A., D.H. Templeton, and A. Zalkin. 1978. *Inorganic Chemistry* 8: 2317.
- [67] Brady, Erik D., David L. Clark, John C. Gordon, P. Jeffery Hay, D. Webster Keogh, Rinaldo Poli, Brian L. Scott, and John G. Watkin. 2003. "Tris(bis(trimethylsilyl)amido) samarium: X-ray Structure and DFT Study." *Inorganic Chemistry* 42: 6682-6690.
- [68] Ghotra, J.S., M.B. Hursthouse, and A.J. Welch. 1973. *Journal of the Chemical Society Chemical Communications*: 669.
- [69] Hitchcock, Peter B., Alexander G. Hulkes, Michael F. Lappert, and Zhengning Li. 2004. "Cerium(III) dialkyl dithiocarbamates from $[\text{Ce}\{\text{N}(\text{SiMe}_3)_2\}_3]$ and tetraalkylthiuram disulfides, and $[\text{Ce}(\kappa^2\text{-S}_2\text{CNET}_2)_4]$ from the Ce^{III} precursor; Tb^{III} and Nd^{III} analogues." *Dalton Transactions* 129-136.
- [70] Hermann, W.A., R. Anwander, F.C. Munck, W. Scherer, V. Dufaud, N.W. Huber, and G.R.J. Artus. 1994. *Zeitschrift für Naturforschung* B49: 1789.
- [71] Bienfait, André M., Benjamin M. Wolf, Karl W. Törnnoos, and Reiner Anwander. 2018. "Trivalent Rare-earth-Metal Bis(trimethylsilyl)amide Halide Complexes by Targeted Oxidations." *Inorganic Chemistry* 57: 5204-5212.
- [72] Niemeyer, Mark. 2002. "Synthese und strukturelle Charakterisierung verschiedener Ytterdiumbis(trimethylsilyl)amide darunter σ -donorfrees $[\text{Yb}\{\text{N}(\text{SiMe}_3)_2\}_2(\mu\text{-Cl})]_2$ – Ein koordinativ ungesättigter Komplex mit zusätzlichen agostischen $\text{Yb}\cdots(\text{H}_3\text{C-Si})$ Wechselwirkungen." *Zeitschrift für Anorganische und Allgemeine Chemie* 628: 647-657.
- [73] Anwander, R. 1992. Thesis. Technical University, Munich.
- [74] Westerhausen, M., M. Hartmann, A. Pfitzner, and W. Schwarz. 1995. *Zeitschrift für Anorganische und Allgemeine Chemie* 621:837.

- [75] Stewart, Joanne L. and Richard A. Andersen. 1998. "Trivalent uranium chemistry: molecular structure of $[(\text{Me}_3\text{Si})_2\text{N}]_3\text{U}$." *Polyhedron* 17(5-6): 953-958.
- [76] Gaunt, Andrew J., Alejandro E. Enriquez, Sean D. Reilly, Brian L. Scott, and Mary P. Neu. 2008. "Structural Characterization of $\text{Pu}[\text{N}(\text{SiMe}_3)_2]_3$, a Synthetically Useful Nonaqueous Plutonium(III) Precursor." *Inorganic Chemistry* 47: 26-28.
- [77] Lappert, M.F., J.B. Pedley, G.J. Sharp, D.C. Bradely. 1976. *Journal of the Chemical Society Dalton Transactions*: 1737. Green, J.C., M. Payne, E.A. Seddon, R.A. Andersen. 1982. *Journal of the Chemical Society Dalton Transactions*: 887.
- [78] Bleaney, B., C.M. Dobson, B.A. Levine, R.B. Martin, R.J.P. Williams, and A.V. Xavier. 1972. *Journal of the Chemical Society Chemical Communications* 791.
- [79] Bleaney, B. 1972. *Journal of Magnetic Resonance* 8: 91.
- [80] Le Mar, G.N., W. DeW. Horrocks, Jr., R.H. Holm. 1973. *NMR of Paramagnetic Molecules*. Academic Press, Inc.
- [81] Bertini, Ivano, Claudio Luchinat, Giacomo Parigi, and Enrico Ravera. 2017. *NMR of Paramagnetic Molecules*. Elsevier.
- [82] Boudreaux, E.A. and L.N. Mulay. 1976. *Theory and Applications of Molecular Paramagnetism*. John Wiley & Sons, New York.
- [83] Smiles, Danil E., Guang Wu, Peter Hrobárik, and Trevor W. Hayton. 2016. "Use of ^{77}Se and NMR Spectroscopy to Probe Covalency of the Actinide-Chalcogen Bonding in $[\text{Th}(\text{E}_n)\{\text{N}(\text{SiMe}_3)_2\}_3]$ (E = Se, Te; $n = 1, 2$) and Their Oxo-Uranium(VI) Congeners." *Journal of the American Chemical Society* 138: 814-825.
- [84] Durdađı, Sevil. 2017. "Chemical environment change analysis on *L* X-ray emission spectra of some lanthanide compounds." *Microchemical Journal* 130: 27-32.
- [85] Durdađı, Sevil. 2013. "Effect of applied external magnetic field on the *L* X-ray emission line structures of the lanthanide elements." *Radiation Physics and Chemistry* 92: 1-7.
- [86] Takahashi, Yoshihito. 1972. "The X-ray Emission Spectra of the Compounds of Third-Period Elements. II. The *K* Spectra of Phosphorus in Compounds." *Bulletin of the Chemical Society of Japan* 45(4): 4-7.
- [87] Yumatov, V.D., L.N. Mazalov, and E.A. Il'inchik. 1980. "Electronic Structure of a Series of Organic Compounds of Phosphorous and the Nature of the Chemical Bond Between Phosphorus and Oxygen." *Zhurnal Strukturnoi Khimii* 21(5): 24-28.
- [88] Sugiura, Chikara, Hiroharu Yorikawa, and Shinji Muramatsu. 1996. "*K β* X-Ray Emission Spectra and Chemical Environments of Phosphorus in Some Selected Compounds." *Journal of the Physical Society of Japan* 65(9): 2940-2945.
- [89] Petric, Marko, Rok Bohinc, Klemen Bučar, Matjaž Žitnik, Jakub Szlachetko, and Matjaž Kavčič. 2015. "Chemical State Analysis of Phosphorus Performed by X-ray Emission Spectroscopy." *Analytical Chemical* 87: 5632-5639.
- [90] Blank, H. -R., M. Frank, M. Gełger, J. -M. Greneche, M. Ismaier, M. Kaltenhäuser, R. Kapp, W. Kreische, M. Leblanc, U. Lossen, and B. Zapf. 1994. "Systematic Investigation of MF_3 Crystalline Compounds (M = Al, Cr, Fe, Ga, In, Sc, Ti, and V) and $\text{Fe}_{1-x}\text{M}_x\text{F}_3$ Mixed Series (M = Ga, Cr, V)." *Zeitschrift für Naturforschung* 49a: 361-366.
- [91] Smith, J.A.S. 1986. "Nuclear Quadrupole Resonance: The Present State and Further Development." *Zeitschrift für Naturforschung* 41a: 453-462.
- [92] Frank, Michael. 1999. "On Systematics in the ^{19}F Electric Hyperfine Interactions." *Fortschritte der Physik* 4: 335-388.
- [93] Jingqing, Ren and Xu Guangxian. 1987. "Electronic Structure and Chemical Bonding of Bis(Trimethylsilyl) Amide Derivatives of Lanthanides ($\text{Ln}[\text{N}(\text{SiMe}_3)_2]_3$, Ln = Nd, Eu, Yb)." *Scientia Sinica B* 30(4): 337-346.

Submitted May 1, 2023 Accepted October 30, 2023